Available online at www.sciencedirect.com
SCIENCE DIRECT
Journal of Volcanology and Geothermal Research 153 (2006) 200–220
Journal of volcanology and geothermal research
www.elsevier.com/locate/jvolgeores

Pre-eruptive crystallization conditions of mafic and silicic magmas at the Plat Pays volcanic complex, Dominica (Lesser Antilles)

R. Halama [a,*], G. Boudon [a], B. Villemant [a], J.-L. Joron [b], A. Le Friant [a], J.-C. Komorowski [a]

[a] *Equipe de Volcanologie, Institut de Physique du Globe de Paris et CNRS, case courrier 89, 4 Place Jussieu, 75005 Paris, France*
[b] *Groupe des Sciences de la Terre, Laboratoire Pierre Süe, CE Saclay, 91191 Gif sur Yvette cedex, France*

Received 15 March 2005; received in revised form 24 November 2005; accepted 9 December 2005
Available online 31 January 2006

Abstract

Andesitic to dacitic magmas of the Plat Pays volcanic complex (Dominica, Lesser Antilles) that erupted during the last ~100 ka equilibrated at temperatures of 800–880 °C and total pressures of 1.1–2.3 kbar. Magmatic conditions were moderately oxidizing (f_{O2} ~1.5 ± 0.3 log units above FMQ) and estimated melt water contents vary from 5.2 to 6.5 wt.%. The crystal-rich nature of the samples, the relatively narrow bulk rock compositional range and the similarity of the intensive crystallization parameters throughout the sample suite are consistent with the presence of a long-lived, highly crystallized magma reservoir. Further crystallization during ascent produced highly evolved rhyolitic glass compositions. The silicic magma reservoir was occasionally invaded by more mafic melts of basaltic andesitic to basaltic composition. These were rarely erupted, but they mixed with the silicic magmas and were frequently incorporated as mafic enclaves. The mafic magmas record temperatures of ~1060 °C at f_{O2} = 1.6–2.0 log units above FMQ. The similarities in mineralogy, petrology and inferred magma storage conditions of the Plat Pays volcanic complex with the Soufriere Hills volcano, Montserrat, and Montagne Pelée, Martinique, can serve as a useful guide for forecasting and evaluation of possible future eruptions.

Keywords: Lesser Antilles; Dominica; Plat Pays volcanic complex; petrology; geothermobarometry; QUILF

1. Introduction

Knowledge of the pre-eruptive conditions of subduction-zone magmas is essential for understanding volcanic processes and better evaluating the potential associated hazards. At the Plat Pays volcanic complex (Southern Dominica, Lesser Antilles island arc), fumarolic activity and frequent seismic swarms of volcanic earthquakes indicate the existence of an active magma reservoir at depth (Wadge, 1985; Stasiuk et al., 2002; Lindsay et al., 2003), and it can be considered as a potentially active volcano (Fig. 1). Lindsay et al. (2003) introduced the term "Plat Pays volcanic complex" to describe the southernmost volcanic center on Dominica, which will be referred to as Plat Pays in the following. The complex includes several volcanic domes and the horseshoe-shaped Soufrière depression. Detailed stratigraphy and a compilation of published and new ^{14}C age determinations of volcanic deposits from Plat Pays (Lindsay et al., 2003) confirm Wadge's (1985) findings that the most recent volcanism on Dominica occurred 685 ± 55 years B.P. from the

* Corresponding author. Department of Geology, University of Maryland, College Park, MD, 20742, USA. Fax: +1 301 405 3597.
E-mail address: rhalama@geol.umd.edu (R. Halama).

0377-0273/$ - see front matter © 2006 Elsevier B.V. All rights reserved.
doi:10.1016/j.jvolgeores.2005.12.001

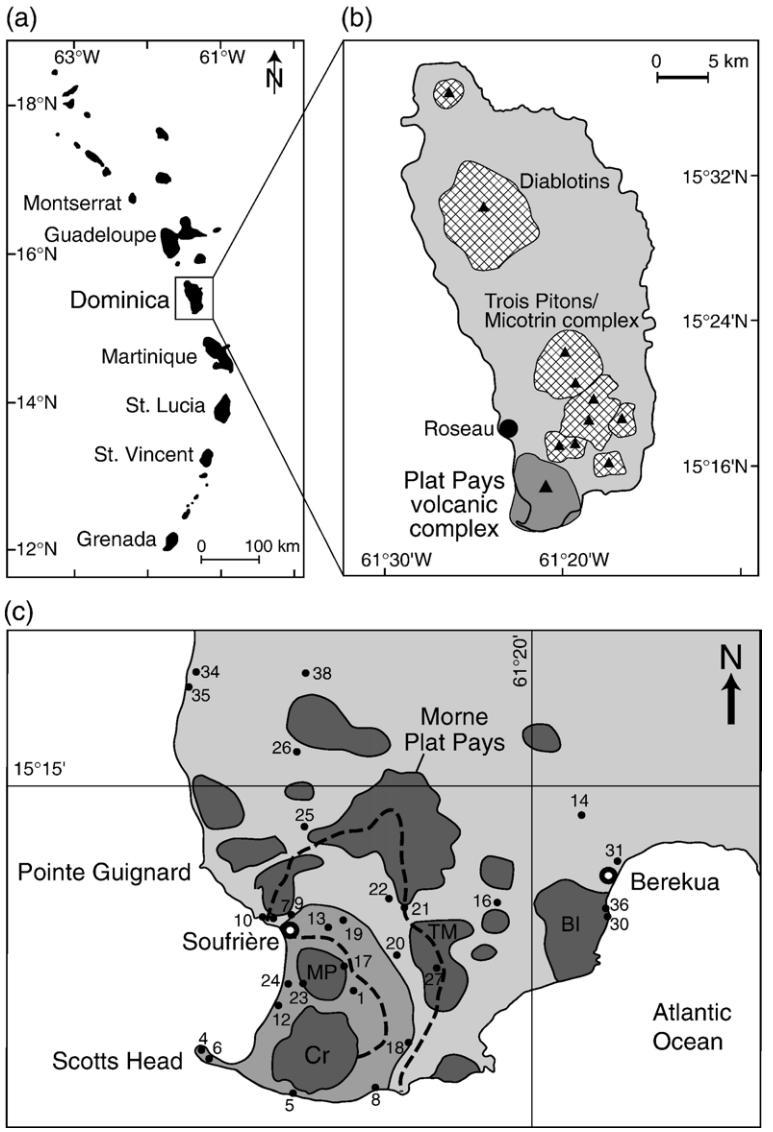

Fig. 1. (a) Simplified map of the Lesser Antilles arc. (b) Map of Dominica after Lindsay et al. (2003) with the location of the Plat Pays complex (dark grey) and other volcanic centers (cross-hatched pattern). (c) Sample locations on a simplified geological map (modified after Le Friant et al. (2002) and Lindsay et al. (2003)). Only the sample numbers are given, prefix for all samples is DOM. Dark grey areas are volcanic lava domes (MP=Morne Patates, TM=Tête Morne, Cr=Crabier, BI=Bois d'Inde), medium grey is the area of recent volcanism. Dashed lines indicate flank-collapse scarps.

Morne Patates dome in the southern part of Plat Pays. The exposed volcanic deposits are dominated by block-and-ash flows (BAFs) that were most likely generated by collapse of actively growing lava domes, similar to those formed during the 1902 and 1929 eruptions of Montagne Pelée on Martinique (Lacroix, 1904; Perret, 1937) and the 1995–2003 eruption of Soufriere Hills, Montserrat (e.g. Young et al., 1998; Druitt and Kokelaar, 2002). Minor pyroclastic flow and fall deposits and dome carapace breccias interfinger with the BAF deposits. The most voluminous ash-and-pumice flow deposit, the Grand Bay ignimbrite, is dated at ~39,000 years B.P. (Lindsay et al., 2003). Based on submarine geophysical and on land field data, Le Friant et al. (2002) identified three major flank-collapse events in the history of the complex, one of which formed the Soufrière depression between 6600 and 2380 years B.P. Flank collapse events played an important role in the development of Plat Pays, as evidenced by the extensive debris-avalanche deposits on land and off the

southwest coast (Deplus et al., 2001; Le Friant et al., 2002). The youngest flank collapse event occurred between 2380 and 685 years B.P., whereas an older event is thought to have taken place at >100,000 years B.P. (Le Friant et al., 2002).

Although several general studies of the Lesser Antilles include data of rocks from Dominica (e.g. Brown et al., 1977; Arculus and Wills, 1980; White and Dupré, 1986), very few studies have been carried out on the petrology and geochemistry of specific volcanic centers on Dominica except for two papers on the recent volcanism on Southern Dominica by Lindsay et al. (2005) and Gurenko et al. (2005). Since there are several settlements within close distance of Plat Pays, more investigations are necessary to better understand the behavior of this particular volcano and to evaluate the volcano's potential activity in hazard assessment. As on Montserrat, where the Soufrière Hills volcano became active in 1995 after a ~350-year long period of dormancy (Young et al., 1998), activity at Plat Pays after a long repose period is conceivable, if not likely. In this study, we use thermobarometry and mineral chemistry of phenocryst assemblage(s) to quantify pre-eruptive crystallization conditions of the Plat Pays magmas. A model of magma storage conditions is proposed and compared to other volcanoes of the Lesser Antilles arc.

2. Location and samples

Dominica is part of the Central Lesser Antilles arc (Fig. 1a), which formed as a consequence of the westward subduction of the North American Plate beneath the Caribbean Plate. The Plat Pays complex is located in the south of the island, near the capital Roseau (Fig. 1b). Studied samples range in age from >100,000 years B.P. (Le Friant et al., 2002) to ~685 years B.P. (Lindsay et al., 2003). Thus, the sample set includes samples from the volcanic complex that existed before the first inferred flank collapse event to the most recent lava domes. The analyzed samples are mainly dense dome fragments from undated block-and-ash flow deposits. Pumice from ash-and-pumice flow deposits, scoria and mafic enclaves from host dacites/andesites have also been analyzed. One mafic scoria (DOM-38) is from a coarse scoria air fall deposit on top of a finer grained scoria fall deposit intercalated with scoriaceous surge deposits. The entire scoriaceous pyroclastic sequence, located close to the Fond Baron Estate at the road between Berekua and Loubière, overlies a sequence of block-and-ash flow deposits. Sample locations are shown in Fig. 1c. Using the age constraints given by the flank-collapse events as described in Le Friant et al. (2002), 12 of the 36 samples analyzed are younger than 6600 years B.P. All samples were analyzed for major and trace elements, including 2 mafic enclaves separated from their host rocks (DOM-8d and DOM-34e) and 3 scoriaceous samples (DOM-8a, DOM-$14b_1$ and DOM-38). A total of 20 thin sections were made, of which samples representative for the textural and mineralogical variations were prepared for electron microprobe analysis. Three of those comprise mafic enclaves (DOM-8d, DOM-26b and DOM-34b/e), but enclaves occurred in other samples as well. Although there are significant temporal gaps between the samples investigated and despite difficulties to establish a complete record of eruptions due to dense vegetation and lack of outcrops, the sample suite is thought to be fairly representative for the eruptions in the time-span under consideration. We also looked for temporal variations in the geochemistry of the samples, but it was not possible to identify clear trends or distinct differences. Therefore, we think it is justified to draw general conclusions on the magma reservoir of the Plat Pays volcanic complex.

3. Analytical methods

Whole-rock major element contents were determined by ICP–AES at the Service d'Analyse des Roches et des Minéraux, CRPG–CNRS, Vandoeuvre-lès-Nancy (France), using a Jobin-Yvon JY 70 instrument. Typical errors are <1% for Si, Al and Fe, <2% for Mn, Ca, Na and K and <10% for Mg and Ti. Trace element concentrations were determined by INAA using the OSIRIS reactor at the Centre d'Etudes de Saclay (France), following a method described by Joron et al. (1997). Detection limits range from 0.5 ppb (Ta) to 1.5 ppm (Zr). Errors, based on repeated analysis of the geochemical standard BEN, are typically <3.5% (Joron et al., 1997). Mineral and glass analyses were carried out using Cameca SX 50 and SX 100 electron microprobes at the Service d'Analyse CAMPARIS, Paris. Analytical conditions were 10 nA beam current and 15 kV acceleration voltage. Various natural and synthetic silicates and oxides were used as standards, and a PAP (Pouchou and Pichoir, 1985) correction procedure was employed. For glass analyses, a defocused beam to minimize Na loss was applied. Peak counting times were usually 10 or 15 s depending on the element and mineral analyzed, and analytical uncertainty is typically <1% for major elements.

4. Petrography, mineral and glass chemistry

4.1. Andesites and dacites

The andesitic and dacitic dome fragments from BAF deposits as well as the pumice samples are highly crystalline with 49–63 wt.% phenocrysts and microphenocrysts (calculated on a bubble-free basis). The proportion of large crystals (>500 μm) is relatively high (>25% in a typical thin section, determined using the NIH Image software). The phenocryst assemblage consists of plagioclase (36–44%), orthopyroxene (6–10%), amphibole (0–13%), titanomagnetite (1.9–2.9%), clinopyroxene (<1%), and accessory apatite. Ilmenite is rare and mainly

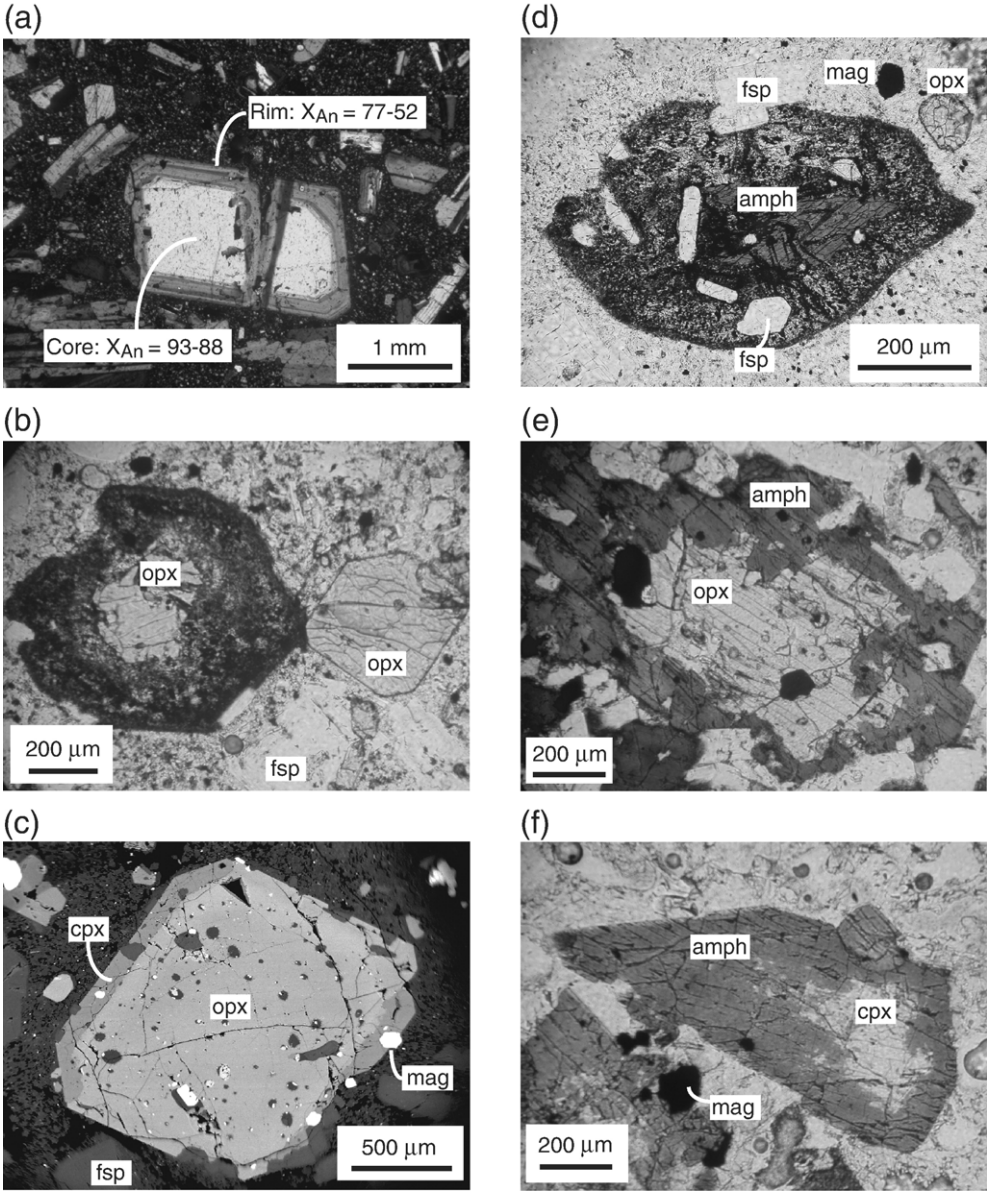

Fig. 2. Images of thin sections from Plat Pays rocks. (a), (b) and (d)–(f) are photomicrographs ((a) is with crossed polars), (c) is a back-scattered electron image; fsp = feldspar, opx = orthopyroxene, cpx = clinopyroxene, mag = titanomagnetite, amph = amphibole; (a) Feldspar crystal with highly calcic core (DOM-12). (b) Two orthopyroxene crystals. Note the thick reaction rim of the crystal on the left hand side (DOM-34a). (c) Orthopyroxene with clinopyroxene overgrowth (DOM-8c). (d) Amphibole with thick reaction rim consisting of plagioclase, titanomagnetite and pyroxene. (DOM-1). (e) Amphibole overgrowth over orthopyroxene within a mafic enclave (DOM-8d). (f) Amphibole with remnant core of clinopyroxene within a mafic enclave (DOM-8d).

occurs as inclusion in pyroxenes. Slightly rounded quartz crystals were found in one dacitic sample (DOM-34b). Microlites (<~100 μm) in the groundmass comprise plagioclase, pyroxenes and Fe–Ti oxides. A continuous grain size distribution of crystals is observed from microlites to phenocrysts for plagioclase and the pyroxenes, but amphibole occurs predominantly as large (>500 μm) phenocrysts. Matrix glass is usually absent in the dense dome fragments but relatively more abundant in pumice and scoria samples. Glass inclusions occur frequently in plagioclase and orthopyroxene in all types of samples. The observed mineral compositional variations predominantly occur on hand-specimen scale, but systematic changes on the sample set scale are lacking. Variations between different mafic phenocrysts within a given sample are usually greater than those observed within a single crystal.

Plagioclase textures vary widely within the same thin section and normal, reverse and oscillatory zoning patterns occur. The compositional range within a single thin section can be significant and the overall range is An_{48}–An_{93} (An=100 Ca/[Ca+Na+K]). Some plagioclase phenocrysts contain dusty sieve-textures, whereas others have cores with relatively constant anorthite contents between 88 and 93 mol% (Fig. 2a).

Orthopyroxene (opx) is the most common mafic mineral. Orthopyroxene phenocrysts are often euhedral (Fig. 2b), but subhedral crystals with overgrowths of clinopyroxene are not uncommon (Fig. 2c). Reaction zones around orthopyroxene phenocrysts are relatively rare and they occur together with euhedral crystals (Fig. 2b). In other samples, orthopyroxene cores overgrown by amphibole are observed. Compositions of most orthopyroxenes from andesitic and dacitic samples fall into a narrow compositional range (Fig. 3). Only few crystals plot largely outside of this range. Orthopyroxene cores have Mg# (100 Mg/[Mg+Fe^{2+}]) between 50 and 67 and Wo (Ca/[Ca+Mg+Fe^{2+}]) between 0.015 and 0.036 (Table 1, Fig. 3). For the crystals analyzed, there is no obvious correlation between crystal size and composition. Rim compositions generally overlap with core compositions, but a few crystals with normal core to rim chemical zoning were also observed. Some of the orthopyroxene surrounded by clinopyroxene show relatively Mg-rich compositions (Mg#=62–63). Al_2O_3 concentrations vary between 0.30 and 2.27 wt.%.

Clinopyroxene (cpx) phenocrysts and microphenocrysts, and clinopyroxene partly or completely surrounding orthopyroxene, are euhedral to subhedral. The bulk of the analyses, independent of crystal size or position within the crystal, define a rather narrow compositional field (Fig. 3). Mg# varies between 60 and 74 and Wo between 0.41 and 0.48 (Table 1). Concentration ranges of Al_2O_3 and TiO_2 are 0.8–4.4 and 0.08–0.73 wt.%, respectively. As for orthopyroxene, large departures from the main compositional do-

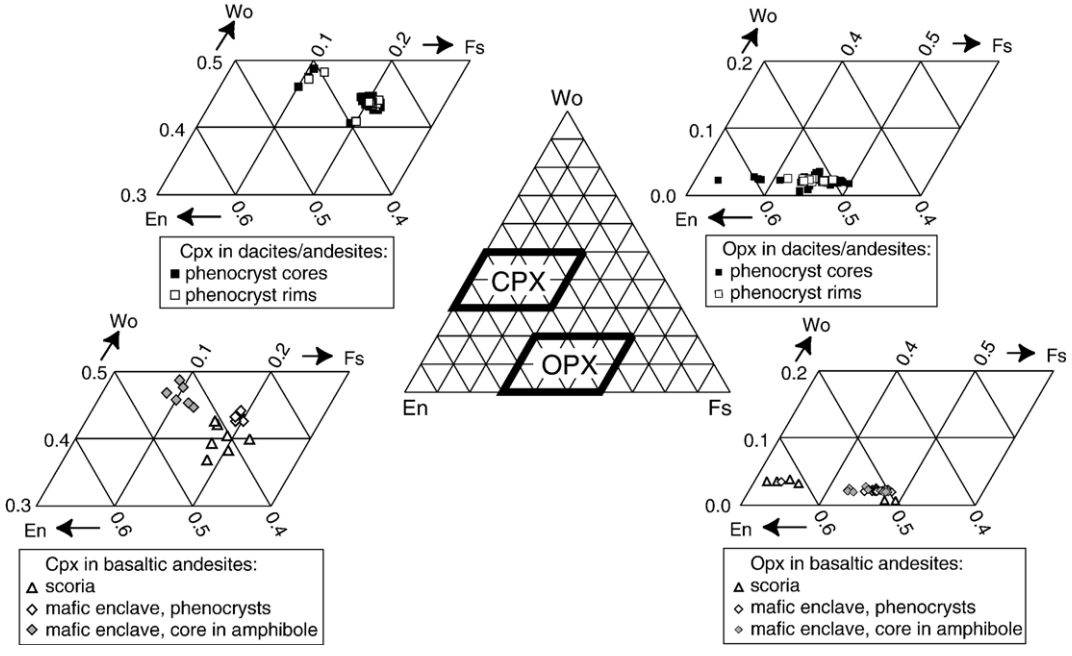

Fig. 3. Composition of clinopyroxenes and orthopyroxenes from Plat Pays rocks, plotted in the En–Fs–Wo triangle (En=Mg, Fs=Fe^{2+}+Fe^{3+}+Mn, Wo=Ca).

Table 1
Representative pyroxene compositions of Plat Pays rocks, determined by electron microprobe

Sample	DOM-1	DOM-31	DOM-36	DOM-38	DOM-8d	DOM-26b	DOM-8a	DOM-12	DOM-31	DOM-38	DOM-8d	DOM-26b
Rock type	Dacite	Dacite	Andesite	Basaltic andesite	Mafic enclave	Mafic enclave	Dacite	Dacite	Dacite	Basaltic andesite	Mafic enclave	Mafic enclave
Mineral	opx	opx	opx	opx	opx	opx	cpx	cpx	cpx	cpx	cpx	cpx
Comment	Core	Rim	Core	Core	Core in amphibole	Core	Core	Rim	Core	Core	Core in amphibole	Core
SiO_2	51.65	52.66	52.24	52.46	52.10	51.77	52.24	51.61	52.45	51.90	52.36	51.63
TiO_2	0.10	0.07	0.12	0.30	0.10	0.17	0.34	0.15	0.28	0.61	0.61	0.42
Al_2O_3	0.37	0.69	0.65	1.93	0.57	0.68	0.95	0.95	1.22	2.91	5.17	4.05
Cr_2O_3	0.01	0.03	0.00	0.00	0.00	0.03	0.02	0.05	0.06	0.00	0.83	0.21
FeO	27.99	26.57	25.89	20.45	25.13	26.85	12.42	12.61	11.27	10.69	5.54	6.03
MnO	1.27	0.78	1.10	0.67	1.06	1.00	0.31	0.70	0.45	0.26	0.14	0.15
MgO	17.47	18.87	18.71	22.89	19.02	18.48	12.40	12.08	13.24	14.85	13.50	15.10
CaO	1.14	1.20	1.18	1.79	1.03	1.01	20.91	21.36	21.00	19.01	21.14	22.00
Na_2O	0.01	0.00	0.02	0.10	0.04	0.03	0.23	0.24	0.26	0.32	0.48	0.25
Total	100.01	100.87	99.89	100.60	99.04	100.02	99.82	99.74	100.23	100.53	99.77	99.84
Formulae based on 4 cations and 6 oxygens:												
Si	1.99	1.99	1.99	1.93	2.00	1.98	1.98	1.96	1.97	1.92	1.93	1.90
Al	0.02	0.03	0.03	0.08	0.03	0.03	0.04	0.04	0.05	0.13	0.22	0.18
Ti	0.00	0.00	0.00	0.01	0.00	0.00	0.01	0.00	0.01	0.02	0.02	0.01
Cr	0.00	0.00	0.00	0.00	0.00	0.00	0.00	0.00	0.00	0.00	0.02	0.01
Fe^{3+}	0.00	0.00	0.00	0.05	0.00	0.01	0.00	0.05	0.02	0.02	0.00	0.01
Mg	1.00	1.06	1.06	1.25	1.09	1.05	0.70	0.68	0.74	0.82	0.74	0.83
Fe^{2+}	0.90	0.84	0.83	0.57	0.81	0.85	0.39	0.35	0.33	0.31	0.17	0.17
Mn	0.04	0.02	0.04	0.02	0.03	0.03	0.01	0.02	0.01	0.01	0.00	0.00
Ca	0.05	0.05	0.05	0.07	0.04	0.04	0.85	0.87	0.84	0.75	0.84	0.87
Na	0.00	0.00	0.00	0.01	0.00	0.00	0.02	0.02	0.02	0.02	0.03	0.02
Total	4.00	4.00	4.00	4.00	4.00	4.00	4.00	4.00	4.00	4.00	4.00	4.00
Mg#	53	56	56	69	57	55	64	66	69	73	81	83
Wo	0.024	0.025	0.024	0.036	0.021	0.021	0.435	0.440	0.432	0.394	0.476	0.460
En	0.503	0.538	0.539	0.635	0.552	0.531	0.359	0.346	0.379	0.428	0.424	0.439
Fs	0.473	0.438	0.436	0.329	0.427	0.449	0.207	0.214	0.188	0.177	0.100	0.101

Mg#=100 Mg/(Mg+Fe^{2+}); Wo, En and Fs are calculated after Morimoto et al. (1988): Wo≡Ca, En≡Mg, Fs≡Fe^{2+}+Fe^{3+}+Mn; note that these values can be slightly different to those calculated by QUILF.

main may be observed for few particular crystals. For example, elevated Al_2O_3 concentrations (up to 2.9 wt.%) are exclusively found in clinopyroxene rims around orthopyroxene, whereas the composition range of individual crystals is 0.9–1.3 wt.%. Clinopyroxenes of reaction zones around amphibole also display elevated Al_2O_3 (2.0–2.2 wt.%) and TiO_2 (0.52–0.73 wt.%) concentrations.

Amphibole occurs as large (up to 1 cm), euhedral to rounded, brown phenocrysts. In a same thin section, other amphibole crystals may be surrounded by thick reaction rims (up to 300 μm), consisting of plagioclase, clinopyroxene and titanomagnetite (Fig. 2d). Amphibole phenocrysts are magnesio-hornblendes (nomenclature after Leake et al., 1997). Mg# and Al_2O_3 ranges are 55–67 and 5.9 to 8.1 wt.%, respectively (Table 2). Rare amphiboles with ~12 wt.% Al_2O_3 are also present. The bulk of the amphiboles have an A-site occupancy (Na+K per formula unit) of 0.2 to 0.4, but some crystals reach values of up to 0.7 (Fig. 4). Cl concentrations range from 0.08 to 0.24 wt.%.

Titanomagnetite phenocrysts ($Mt_{66–73}$) are subhedral, and some of them show oxy-exsolution lamellae of ilmenite. Representative analyses of titanomagnetite are presented in Table 3. Single ilmenite crystals ($Ilm_{83–92}$) are scarce, and magnetite and ilmenite in contact can rarely be found.

Glass inclusions in andesitic and dacitic samples are, without exception, rhyolitic (Table 4, Fig. 5) with SiO_2 contents (anhydrous) between 74.8 and 83.8 wt.%. Water contents, determined using the 'by difference' method from electron microprobe analyses (100% − (Sum of oxides+Cl)=H_2O) (Devine et al., 1995), range between 0 and 7 wt.%. Matrix glass compositions could only be measured in one andesitic scoria (DOM-14b_1). Their anhydrous composition (75.0–78.3 wt.% SiO_2) and

Table 2
Representative amphibole compositions of Plat Pays rocks, determined by electron microprobe

Sample	DOM-1	DOM-1	DOM-8a	DOM-8c	DOM-14b1	DOM-14b1	DOM-14b1	DOM-8d	DOM-8d	DOM-8d
Rock type	Dacite	Dacite	Dacite	Dacite	Andesite	Mafic enclave	Mafic enclave	Mafic enclave	Mafic enclave	Mafic enclave
Amphibole name[a]	Edenite	Mg-hbl	Mg-hbl	Mg-hbl	Mg-hbl	Mg-hastingsite	Pargasite	Mg-hastingsite	Tschermakite	Tschermakite
Comment		With corona		Rim around opx		Green	Green			
SiO_2	47.67	48.03	46.56	47.57	47.09	41.06	41.21	44.34	44.04	43.36
TiO_2	1.49	1.64	2.04	1.65	1.63	1.91	2.03	2.42	2.23	1.99
Al_2O_3	7.02	7.16	7.17	7.37	7.23	13.43	13.00	10.95	10.73	10.92
Cr_2O_3	0.05	0.00	0.03	0.04	0.00	0.18	0.00	0.00	0.05	0.06
FeO	15.89	17.24	17.45	16.94	17.28	15.59	15.97	12.61	14.60	14.89
MnO	0.30	0.44	0.23	0.13	0.37	0.34	0.25	0.09	0.29	0.44
MgO	12.31	11.62	11.37	12.22	11.75	10.87	10.61	14.09	13.17	13.08
CaO	11.11	10.30	10.87	11.02	10.92	11.35	11.35	11.68	11.00	10.57
Na_2O	2.93	1.50	1.29	1.42	1.35	2.15	2.15	1.93	1.79	2.02
K_2O	0.32	0.27	0.33	0.31	0.26	0.27	0.26	0.32	0.37	0.42
Cl	0.11	0.11	0.18	0.13	0.17	0.04	0.03	0.05	0.04	0.09
F	0.41	0.08	0.35	0.40	0.24	0.00	0.32	0.45	0.01	0.00
Total	99.09	98.20	97.33	98.67	97.88	97.14	96.83	98.43	98.26	97.75
Formulae and Fe^{3+} content[a]:										
Si	6.97	7.02	6.91	6.93	6.93	6.11	6.17	6.40	6.39	6.33
Al(IV)	1.03	0.98	1.09	1.07	1.07	1.89	1.83	1.60	1.61	1.67
Al(VI)	0.18	0.25	0.16	0.19	0.18	0.46	0.46	0.26	0.23	0.21
Ti	0.16	0.18	0.23	0.18	0.18	0.21	0.23	0.26	0.24	0.22
Fe^{3+}	0.09	0.44	0.37	0.39	0.41	0.51	0.44	0.41	0.62	0.74
Cr	0.01	0.00	0.00	0.00	0.00	0.02	0.00	0.00	0.01	0.01
Mg	2.69	2.53	2.52	2.65	2.58	2.41	2.37	3.03	2.85	2.85
Fe^{2+}	1.85	1.67	1.80	1.67	1.71	1.43	1.56	1.11	1.15	1.08
Mn	0.04	0.05	0.03	0.02	0.05	0.04	0.03	0.01	0.04	0.05
Ca	1.74	1.61	1.73	1.72	1.72	1.81	1.82	1.81	1.71	1.65
Na (B-site)	0.24	0.27	0.17	0.17	0.16	0.10	0.10	0.10	0.15	0.19
Na (A-site)	0.59	0.16	0.20	0.23	0.22	0.52	0.53	0.44	0.35	0.38
K	0.06	0.05	0.06	0.06	0.05	0.05	0.05	0.06	0.07	0.08
Mg#	59	60	58	61	60	63	60	73	71	72

[a] Amphibole names and calculation of formulae after Leake et al. (1997) Mg-hbl = magnesio-hornblende, Mg-hastingsite = magnesio-hastingsite; note that $Al^{VI} < Fe^{3+}$ for Mg-hastingsite, whereas $Al^{VI} > Fe^{3+}$ for pargasite. Mg# = 100 Mg/(Mg + Fe″).

water contents (0.6–2.4 wt.%) are similar to those of the glass inclusions.

4.2. Basaltic andesites: mafic enclaves and vesiculated scoria

Mafic enclaves represent a minor (~1–3%) component of many dacites and have sharply defined smooth or crenulated contacts with the host. They are fine-grained, often ellipsoidal and 0.5 to 20 cm in size. Two types can be defined. (i) Enclaves dominated by plagioclase ($An_{47–81}$) and acicular amphibole (sample DOM-8d). Some of the amphiboles contain cores of orthopyroxene (Fig. 2e) or clinopyroxene (Fig. 2f). The amphibole compositions partly overlap with the compositions of the magnesio-hornblendes from the host rock. They trend towards tschermakitic and magnesio-hastingsitic compositions with higher Al^{IV}, Al^{VI} and (Na + K) per formula unit (Fig. 4). Al_2O_3 contents range from 6.7 to 12.7 wt.% and Cl contents fall between 0.03 and 0.12 wt.%. The orthopyroxene cores in amphibole have Mg# between 55 and 60 and Wo between 0.020 and 0.028 and are similar in composition to rare individual crystals in these enclaves (Mg# = 52–58, Wo = 0.021–0.023) and to the orthopyroxenes from the host rock. However, clinopyroxene cores in amphibole are considerably more Mg-rich (Mg# = 81–85), higher in Al_2O_3 (2.6–5.2 wt.%) and TiO_2 (0.45–0.61 wt.%). (ii) Enclaves with randomly orientated, rather fine-grained crystals, predominantly consisting of plagioclase with variable core compositions

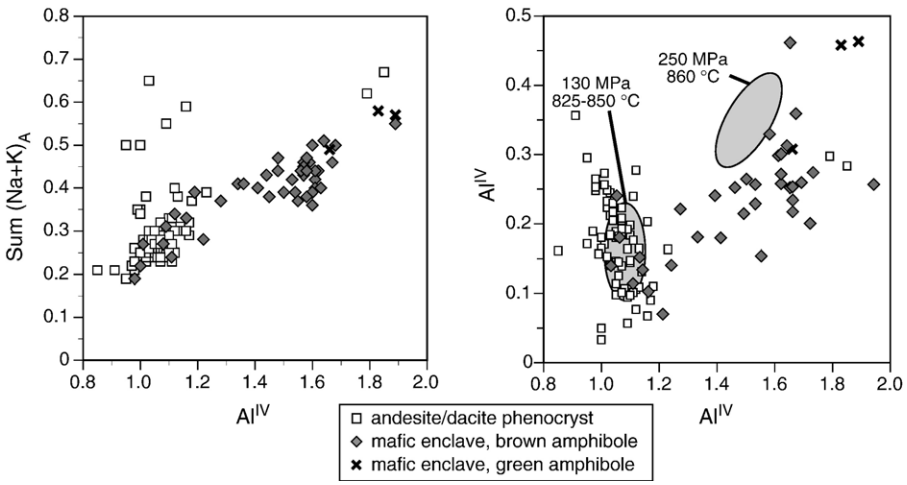

Fig. 4. Composition of amphiboles from Plat Pays rocks: (a) Na+K on A-site vs. Al on tetrahedral site (Al^{IV}). (b) Al in octahedral coordination (Al^{VI}) vs. Al^{IV}; experimental data are from Rutherford and Devine (2003).

($An_{48–85}$), orthopyroxene (Mg#=51–67, Wo=0.008–0.035) and clinopyroxene (Mg#=83–87, Wo=46–51) with lesser amounts of amphibole and subordinate titanomagnetite ($Mt_{58–68}$) (enclaves in samples DOM-26b and DOM-34e). Al_2O_3 concentrations are quite variable (0.4–3.7 wt.%) in orthopyroxenes and relatively high (4.0–6.7 wt.%) in clinopyroxene. Clinopyroxene compositions tend to higher TiO_2 (0.42–0.91 wt.%) and Wo values (0.46–0.51) than the clinopyroxene from the dacites/andesites. Both brown magnesio-hornblendes with Al_2O_3 ~7 wt.% and green amphibole (magnesio-hastingsite/pargasite) with elevated Al_2O_3 contents (11.1–13.4 wt.%) and low Cl concentrations (0.03–0.06 wt.%) are present.

Except for the mafic enclaves, there is only one sample of basaltic andesitic composition in the sample suite (DOM-38). It is an undated scoria from a fall deposit with relatively abundant matrix glass and contains plagioclase, clinopyroxene, orthopyroxene and titanomagnetite ± ilmenite, but no amphibole. Compositions of plagioclase microlites and phenocrysts (up to 300 μm) range between An_{48} and An_{80}. Rare, very large plagioclase crystals (>1 mm) are characterized by highly calcic (An_{96}), unzoned cores. Orthopyroxene is more Ca-rich (Mg#=53–69, Wo=0.033–0.040) and generally higher in Al_2O_3 (1.2–2.2 wt.%) than in the silicic rocks. Clinopyroxene (Mg#=69–76) is more common than orthopyroxene and has elevated Al_2O_3 (1.9–4.2 wt.%) and TiO_2 (0.42–0.92 wt.%) concentrations compared to clinopyroxene from dacites/andesites, whereas Wo contents (0.37–0.44) are lower (Table 1, Fig. 3). Titanomagnetite ($Mt_{49–65}$) is abundant, mainly as individual crystals but also overgrowing the scarce ilmenite ($Ilm_{84–86}$). Matrix glass is of rhyolitic composition (71.5–72.9 wt.% SiO_2, anhydrous), and water contents give 3.1–4.0 wt.%.

5. Geochemistry

Representative whole-rock data are presented in Table 5. The dome fragments and the pumice clasts are of relatively constant, silicic andesitic to dacitic composition (~60–64 wt.% SiO_2, Mg#=42–57) (Fig. 5). The pumiceous samples plot in the more silicic part of this range. One scoria (Mg#=55; sample DOM-38) and the mafic enclaves are of basaltic andesitic composition. CIPW mineral modes in dacites/andesites are mostly uniform and all samples are quartz-normative, although mineral zoning and textures reveal a high degree of complexity in individual samples.

Incompatible trace elements are well correlated for all samples (e.g. Ba vs. Th, Fig. 6a). The dacites/andesites define the higher end member of this range, whereas both, the basaltic andesite scoria and the mafic enclaves, define the lower, more primitive end member. The compositional variation in incompatible trace element concentrations in the dacites and andesites is very limited (e.g. Ta: 0.23–0.32 ppm, Hf: 2.4–3.2 ppm). Compatible trace elements are negatively correlated with highly incompatible elements (e.g. Sc vs. Th, Fig. 6b). There is a marked kink between the more primitive samples and the evolved andesites and dacites with low Sc contents (Sc: 13–22 ppm). On a N-MORB normalized multi-element plot (Fig. 6c), the sample suite as a whole is characterized by an enrichment of large ion lithophile elements (LILE) compared to light rare earth elements (LREE; Ba_N/La_N=6.5–10.8). Both groups, LILE and LREE, are enriched relative to the

Table 3
Representative titanomagnetite analyses of Plat Pays rocks, determined by electron microprobe

Sample	DOM-8c	DOM-12	DOM-14b1	DOM-31	DOM-36	DOM-38	DOM-38	DOM-8d	DOM-26b
Rock type	Dacite	Dacite	Andesite	Dacite	Andesite	Basaltic andesite	Basaltic andesite	Mafic enclave	Mafic enclave
Comment							Around ilmenite		
SiO_2	0.07	0.03	0.03	0.06	0.08	0.13	0.08	0.04	0.28
TiO_2	9.55	9.51	10.02	10.71	10.28	13.93	17.49	9.87	13.69
Al_2O_3	1.92	1.53	1.74	1.94	1.89	2.38	2.11	1.87	1.36
Cr_2O_3	0.11	0.02	0.14	0.00	0.02	0.09	0.07	0.28	0.08
FeO	82.32	82.24	80.92	80.81	81.98	77.67	74.89	82.57	79.15
MnO	0.44	0.70	0.35	0.53	0.40	0.47	0.46	0.38	0.53
MgO	0.74	0.57	1.14	0.89	0.86	1.89	2.28	0.61	0.80
CaO	0.00	0.00	0.02	0.07	0.02	0.07	0.07	0.04	0.03
Total	95.14	94.60	94.36	95.00	95.53	96.63	97.45	95.65	95.91
Formulae calculated on the basis of 3 cations and 4 oxygens:									
Si	0.00	0.00	0.00	0.00	0.00	0.00	0.00	0.00	0.01
Al	0.08	0.07	0.08	0.09	0.08	0.10	0.09	0.08	0.06
Ti	0.27	0.27	0.28	0.30	0.29	0.38	0.48	0.28	0.39
Cr	0.00	0.00	0.00	0.00	0.00	0.00	0.00	0.01	0.00
Fe^{3+}	1.37	1.39	1.35	1.31	1.34	1.12	0.94	1.36	1.15
Mg	0.04	0.03	0.06	0.05	0.05	0.10	0.12	0.03	0.04
Fe^{2+}	1.21	1.21	1.21	1.23	1.23	1.26	1.34	1.22	1.33
Mn	0.01	0.02	0.01	0.02	0.01	0.01	0.01	0.01	0.02
Ca	0.00	0.00	0.00	0.00	0.00	0.00	0.00	0.00	0.00
Total	3.00	3.00	3.00	3.00	3.00	3.00	3.00	3.00	3.00
Mg#	3.3	2.6	5.0	3.9	3.7	7.6	8.5	2.7	3.2
XUsp	0.28	0.28	0.30	0.32	0.30	0.41	0.50	0.29	0.40
XMt	0.72	0.72	0.70	0.68	0.70	0.59	0.50	0.71	0.60
Parameters for QUILF calculations:									
NTi	0.270	0.271	0.285	0.303	0.289	0.386	0.481	0.279	0.387
NMg	0.040	0.031	0.062	0.048	0.046	0.100	0.120	0.033	0.044
NMn	0.014	0.022	0.011	0.017	0.013	0.015	0.014	0.012	0.017

high field strength elements (HFSE; Ba_N/Hf_N=24–36; La_N/Hf_N=2.7–4.1). There is a large negative Ta anomaly and small negative P and Ti anomalies, which are typical of calc-alkaline suites. Dacites and andesites have nearly identical patterns with very similar concentrations. Both the basaltic andesite and the mafic enclave have also similar patterns. The latter two show a slight relative depletion in Zr, Hf and some LILE (Rb, Ba, Th, U) compared to the more silicic rocks.

6. Intensive crystallization parameters (P, T, f_{O2}) and melt water contents

6.1. Pressure

A minimum pressure estimate can be derived from the stability of amphibole in the magma, which requires $P>1.1$ kbar (if $P_{H2O}=P_{total}$) for andesitic to dacitic whole-rock compositions comparable to the Plat Pays rocks (Rutherford and Hill, 1993; Barclay et al., 1998). The minimum pressure estimate goes up to ~1.6 kbar if temperatures reach 900 °C. Application of the Al-in-hornblende geobarometer (Johnson and Rutherford, 1989) for 73 crystals yields $P=1.7\pm0.6$ kbar, whereby the error of the method (±0.6 kbar) is larger than the error obtained from data dispersion (±0.3 kbar). The range of pressures obtained varies between 0.8 and 2.5 kbar (Fig. 7a). Application of the temperature-dependent calibration for the Al-in-hornblende geobarometer of Anderson and Smith (1995) gives an average of -0.5 kbar, which is not in agreement with the minimum stability limit of amphibole. However, the Plat Pays samples do not meet all required conditions for this barometer, such as the presence of K-feldspar, titanite or quartz. The lack of K-feldspar and titanite does not significantly affect the pressure determinations (Anderson and Smith, 1995). In addition, the samples are quartz-normative and some samples contain quartz crystals, suggesting that they were close to quartz saturation. QUILF (Andersen et al., 1993) calculations of silica

Table 4
Representative analyses of glass inclusions and matrix glasses of Plat Pays rocks

Sample	DOM-8c	DOM-8c	DOM-8c	DOM-26b	DOM-26b	DOM-26b	DOM-31	DOM-36	DOM-14b1	DOM-14b1	DOM-38	DOM-38
Type	GI	GI	GI	GI	GI	GI	GI	GI	MG	MG	MG	MG
Host mineral	plag	plag	opx	opx	opx	plag	opx	opx				
SiO_2	73.53	76.92	76.65	74.09	72.68	72.64	75.52	76.12	73.97	76.66	68.56	70.34
TiO_2	0.19	0.44	0.14	0.04	0.05	0.31	0.11	0.20	0.36	0.36	0.78	0.77
Al_2O_3	12.43	9.97	11.32	14.00	11.01	9.10	12.52	12.84	11.75	11.18	12.51	12.51
FeO	1.49	1.88	1.17	1.63	2.55	2.34	0.74	1.48	3.01	2.39	4.85	4.41
MnO	0.06	0.12	0.05	0.12	0.07	0.04	0.04	0.04	0.06	0.11	0.16	0.10
MgO	0.19	0.26	0.30	0.21	0.16	0.36	0.05	0.10	0.39	0.22	0.76	0.67
CaO	1.37	0.93	1.64	1.63	0.12	1.37	1.75	1.51	1.78	1.26	2.50	2.30
Na_2O	5.45	4.42	3.07	4.12	5.00	4.09	3.52	3.52	3.15	2.88	3.37	2.93
K_2O	2.46	3.13	2.27	3.21	2.98	3.38	2.64	3.18	2.96	2.90	2.42	2.48
Cl	0.15	0.34	0.25	0.18	0.19	0.31	0.19	0.22	0.23	0.13	0.11	0.14
Total	97.31	98.40	96.85	99.21	94.81	93.93	97.09	99.22	97.65	98.07	96.01	96.66
H_2O by difference	2.69	1.60	3.15	0.79	5.19	6.07	2.91	0.78	2.35	1.93	3.99	3.34
Projection parameters[a]*:*												
Qz'	30.9	42.4	42.6	31.6	34.9	42.9	37.6	37.3	37.0	43.9	30.3	34.5
Ab'	54.3	37.2	43.8	52.2	45.2	33.3	47.9	45.4	46.3	38.4	57.1	51.2
Or'	14.8	20.3	13.6	16.2	19.9	23.8	14.5	17.3	16.7	17.7	12.6	14.3

[a] Projection parameters after Blundy and Cashman (2001); GI=glass inclusion, MG=matrix glass, plag= plagioclase, opx=orthopyroxene.

activity often indicate quartz saturation as well (e.g. for sample DOM-31, $T=840$ °C and $a_{SiO2}=0.96\pm0.06$). The pressures obtained can be regarded as an upper pressure limit, because P is over-estimated if $a_{SiO2}<1$ (Hammer et al., 2000). Taking into account the error of method (±0.6 kbar), 2.3 kbar is the maximum pressure estimate. The results of the Al-in hornblende geobarometry are in agreement with melt inclusion data (~2 kbar, Gurenko et al., 2004). The pressure estimate is also qualitatively consistent with water-saturated phase relations of compositionally similar rocks, as for instance reported for the Mt. St. Helens dacite (Merzbacher and Eggler, 1984; Rutherford et al., 1985; Rutherford and Devine, 1988). Given the arguments presented above, we consider that the likely pressure range is 1.1–2.3 kbar for crystallization of the amphibole-bearing Plat Pays rocks, but it requires experimental corroboration, where the stability and composition of amphibole would be more precisely determined in relation to P–T–P_{H2O}–f_{O2} changes for typical Plat Pays rocks. The pressures can be converted into a depth estimate if we assume $P_{H2O} \cong -P_{lithostatic}$ and $\rho=2600$ kg/m^3, leading to a reservoir depth of 4–9 km. This is in agreement with constraints from seismic signals, thought to result from magma pressurization associated with the Plat Pays and Morne Anglais centers, which indicate a depth of 2–6 km (Lindsay et al., 2003).

6.2. Temperature

Magma temperatures are estimated using the QUILF program (Andersen et al., 1993). Since chemical equilibrium between clinopyroxene and orthopyroxene phenocrysts only exists in a few samples, temperatures have been calculated in the single pyroxene mode for all samples. This procedure requires input of the orthopyroxene core composition only, and QUILF then calculates an equilibrium clinopyroxene composition and a temperature (Murphy et al., 2000). Results are most sensitive to variations of the CaO content in the orthopyroxene. The accuracy of the thermometer is estimated at ±20 °C (Murphy et al., 2000) and the pressure dependence is low (±3–7 °C/kbar). Calculations were carried out at a fixed pressure of 1.5 kbar. The obtained temperature range in the silicic magma is 760–1075 °C (Fig. 7b). However, the majority of the phenocryst core data (85 crystals in 10 samples) fall into a more narrow temperature interval (800–880 °C) with an average temperature of 840±20 °C. This result is consistent with amphibole-plagioclase thermometry (Holland and Blundy, 1994), which yields temperatures in the range 804–857 °C. The presence of amphibole, which has been shown to become unstable in andesites from Montserrat at $T>875$ °C (Barclay et al., 1998), and the lack of biotite, which becomes stable at ~780 °C (Rutherford and Devine, 2003), also constrain the

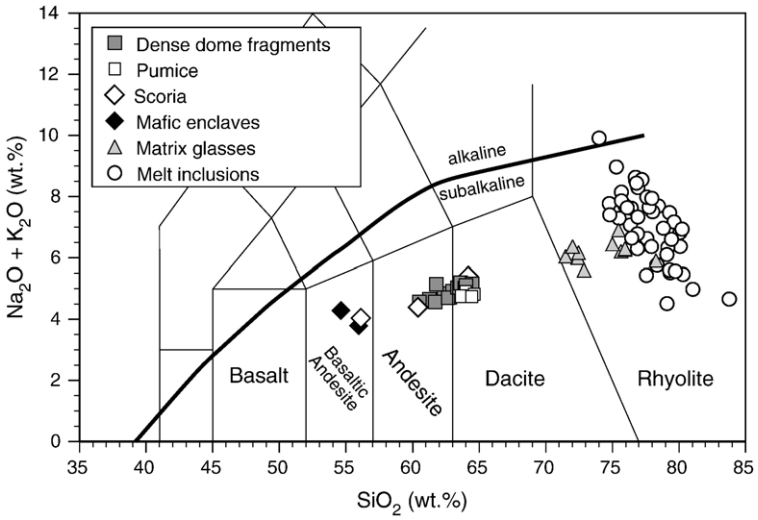

Fig. 5. Composition of whole-rocks, matrix glasses and glass inclusions of the Plat Pays complex in the TAS (Total Alkalies versus Silica) diagram. Analyses were recalculated for all Fe as FeO and normalized to 100% volatile-free. The alkaline–subalkaline subdivision is after Irvine and Baragar (1971).

magma temperature. Orthopyroxenes overgrown by clinopyroxene show slightly more elevated temperatures (904 ± 42 °C, 5 crystals). Temperatures in the mafic enclaves range from 820 to 1050 °C (20 crystals in 3 samples) and average 1058 ± 38 °C (3 crystals) in the scoria (DOM-38). This latter value is considered as representative of the mafic magmas of basaltic andesite composition at Plat Pays since the enclaves are likely to have partly re-equilibrated in the dacitic host magma. Temperatures of ~1060 °C are also in agreement with the lack of amphibole in the scoria, as the upper stability limit of amphibole is 980 °C in basaltic andesite (Sisson and Grove, 1993).

6.3. Oxygen fugacity

Oxygen fugacities are estimated by QUILF using the titanomagnetite compositions with the temperature determined by pyroxene thermometry (Murphy et al., 2000). This method has the advantage that ilmenite, which is only present in very minor abundances, need not be considered in the calculations and problems of rapid re-equilibration of Fe–Ti oxides, particularly ilmenite, are avoided (Murphy et al., 2000). Titanomagnetite reaction rims on ilmenite were not used in the calculations because of possible diffusion gradients (Devine et al., 1998). Results yield oxygen fugacities of 1.2 to 1.8 log units above the FMQ buffer in dacites and mafic enclaves. Slightly higher values are obtained for the basaltic andesite (1.6 to 2 log units above FMQ).

6.4. Constraints from glass compositions

Further constraints on the evolution of the crystallization in the Plat Pays magmas can be derived from the projection of glass compositions onto the Qz–Ar–Or ternary. This procedure allows relative determination of magma equilibration pressure because highly silicic melts (>77 wt.% SiO_2) form as a consequence of contraction of the silica phase volume with decreasing pressure (Cashman and Blundy, 2000; Blundy and Cashman, 2001). Following the method described by these authors, matrix glass and glass inclusion compositions of Plat Pays rocks are displayed in Fig. 8. Matrix glass from the basaltic andesite (sample DOM-38) plots on the Qz-poor side of the 200 MPa water-saturated cotectic (Fig. 8a), whereas matrix glass from an andesite (sample DOM-14b_1) defines a linear trend from the 200 MPa cotectic towards the 0.1 MPa cotectic. Glass inclusions span a broader compositional range on the Qz–Ab–Or diagram (Fig. 8b). Some project on the Qz-poor side of the 300 MPa cotectic, others between the 50 and 0.1 MPa cotectics. All together, they form a roughly linear trend away from Ab towards the 0.1 MPa cotectic, similar to the matrix glass compositions and roughly parallel to the depressurization trend of the ternary minimum. The trends displayed by the glass compositions are qualitatively similar to both the isothermal decompression and the isobaric cooling models from Blundy and Cashman (2001). Importantly, some crystallization must have occurred at very shallow levels within the conduit, because the high Qz contents

Table 5
Representative major and trace element whole-rock analysis of Plat Pays rocks

Sample no.	DOM-6d	DOM-8c	DOM-8d	DOM-12	DOM-13	DOM-14b$_1$	DOM-16	DOM-26a	DOM-31	DOM-34e	DOM-36	DOM-38
Sample type	Pumice	DF	ME	DF	DF	Scoria	DF	DF	Pumice	ME	DF	Scoria
Classification[a]	Dacite	Dacite	BA	Dacite	Dacite	Andesite	Andesite	Andesite	Dacite	BA	Andesite	BA
Major elements (wt.%)												
SiO_2	63.27	63.14	55.12	63.98	63.69	59.35	61.94	60.54	61.84	53.98	60.48	55.18
TiO_2	0.43	0.41	0.85	0.43	0.44	0.50	0.48	0.48	0.45	0.72	0.52	0.67
$Al2O_3$	16.91	17.01	17.57	16.93	17.12	17.46	17.60	18.07	17.06	18.95	17.34	19.40
Fe_2O_3	6.12	6.14	8.23	5.77	5.71	6.89	6.54	6.39	6.13	9.94	6.66	7.81
MnO	0.14	0.14	0.14	0.13	0.14	0.14	0.14	0.14	0.14	0.20	0.14	0.14
MgO	1.75	2.22	4.97	1.97	2.11	3.34	2.26	2.45	1.80	3.94	3.25	3.69
CaO	5.47	5.45	8.68	5.42	5.54	6.84	5.65	6.11	5.64	7.67	6.35	8.18
Na_2O	3.25	3.48	2.80	3.55	3.37	3.09	3.28	3.26	3.12	3.46	3.19	2.92
K_2O	1.41	1.64	0.96	1.57	1.59	1.23	1.50	1.23	1.51	0.76	1.40	1.04
P_2O_5	0.06	0.11	0.13	0.06	0.07	0.09	0.10	0.11	0.09	0.10	0.07	0.06
LOI	0.98	0.07	0.39	−0.01	0.04	0.87	0.32	1.04	1.52	0.10	0.41	0.72
Total	99.79	99.81	99.84	99.80	99.82	99.80	99.81	99.82	99.30	99.82	99.81	99.81
Mg#	44.2	50.1	60.9	48.6	50.6	56.5	48.0	50.6	44.9	50.5	56.6	54.9
Trace elements (ppm)												
Sc	14.1	14.4	27.4	13.5	14.3	21.0	16.4	15.5	14.7	27.1	19.8	26.2
Co	12.5	13.1	24.7	12.0	12.7	18.3	14.8	14.0	12.8	23.1	17.2	22.9
Ni	2.5	2.2	42.3	2.2	2.2	11.6	3.3	2.5	2.6	4.1	14.4	6.0
Zn	66	63	72	61	67	66	67	65	57	99	71	69
Rb	44.2	45.1	27.3	43.8	43.3	35.7	41.2	45.8	45.3	22.5	43	30.2
Sr	228	230	324	220	214	216	233	218	225	268	237	245
Zr	110	94	68	106	95	91	97	104	92	58	86	73
Sb	0.26	0.21	0.17	0.22	0.22	0.23	0.15	0.21	0.28	0.19	0.26	0.20
Cs	2.16	2.25	1.34	2.05	1.53	1.84	0.77	1.25	2.25	0.95	2.09	1.37
Ba	270	275	182	273	272	226	275	284	269	170	258	190
La	11.53	10.93	11.16	11.30	10.94	8.85	12.63	9.74	10.97	9.59	10.28	8.09
Ce	24.7	25.2	29.22	24.10	24.0	20.9	25.0	22.9	23.6	22.8	22.7	19.2
Sm	2.90	2.77	5.44	2.85	2.81	2.58	3.29	2.62	2.83	3.51	2.91	2.71
Eu	0.92	0.96	1.44	0.78	0.82	0.90	1.02	0.92	0.96	1.11	0.86	0.91
Tb	0.441	0.452	0.821	0.436	0.438	0.445	0.488	0.436	0.451	0.570	0.459	0.467
Yb	2.48	2.26	3.61	2.49	2.48	2.19	2.34	2.22	2.2	2.91	2.25	2.3
Hf	2.84	2.86	2.48	2.91	2.78	2.47	2.83	2.97	2.86	1.91	2.57	2.2
Ta	0.279	0.281	0.271	0.293	0.283	0.225	0.292	0.282	0.273	0.218	0.259	0.208
Th	4.20	4.24	2.74	4.27	4.19	3.39	4.36	4.41	4.09	2.16	3.96	3.01
U	1.26	1.23	0.78	1.28	1.24	0.99	1.3	1.26	1.22	0.59	1.14	0.87
W	0.65	0.30	0.56	0.57	0.56	0.25	0.28	0.38	0.44	0.30	0.38	n.d.
As	1.83	1.15	1.69	1.18	1.15	1.26	1.01	1.11	1.43	0.39	1.26	1.02
Mo	0.95	1.00	3.00	0.85	0.88	0.73	1.04	1.08	0.82	0.27	0.80	0.81
Br	4.29	1.14	2.64	0.93	0.52	3.81	1.24	1.08	5.08	0.65	2.56	3.59
Crystallinity (%)	49.1	50.2	–	48.3	47.4	59.6	54.4	56.1	50.9	–	59.4	62.2

[a] The classification is based on the concentrations normalized to 100% volatile-free; n.d.=not detected; Mg#=100 Mg/(Mg+Fe″) in atomic proportions, using Fe_2O_3/FeO ratios recommended by Middlemost (1989); DF=dome fragment, ME=mafic enclave, ves.=vesiculated, BA=basaltic andesite. Crystallinity is expressed as the weight fraction of phenocrysts. It is estimated by mass balance calculation using phenocryst, glass and whole-rock compositions. Average glass and phenocrysts compositions were used in the calculations for most of the samples, except DOM-38 were more mafic compositions for both glass and phenocrysts, as determined by microprobe, were used. The general accuracy of the method was tested by comparing mass-balance calculations to point-counting measurements (Villemant and Boudon, 1998), and the values stated here are in agreement with petrographic observations. Mean propagated error is estimated to be ~5%.

of the most evolved glasses can only be attained at low final crystallization pressures (Cashman and Blundy, 2000). The observed range in glass compositions implies that crystallization occurred at a range of effective pressures. For the differences in the matrix glass composition between the scoria samples DOM-38 and DOM-14b$_1$, this might be related to different ascent rates, because magmas that ascend the most rapidly

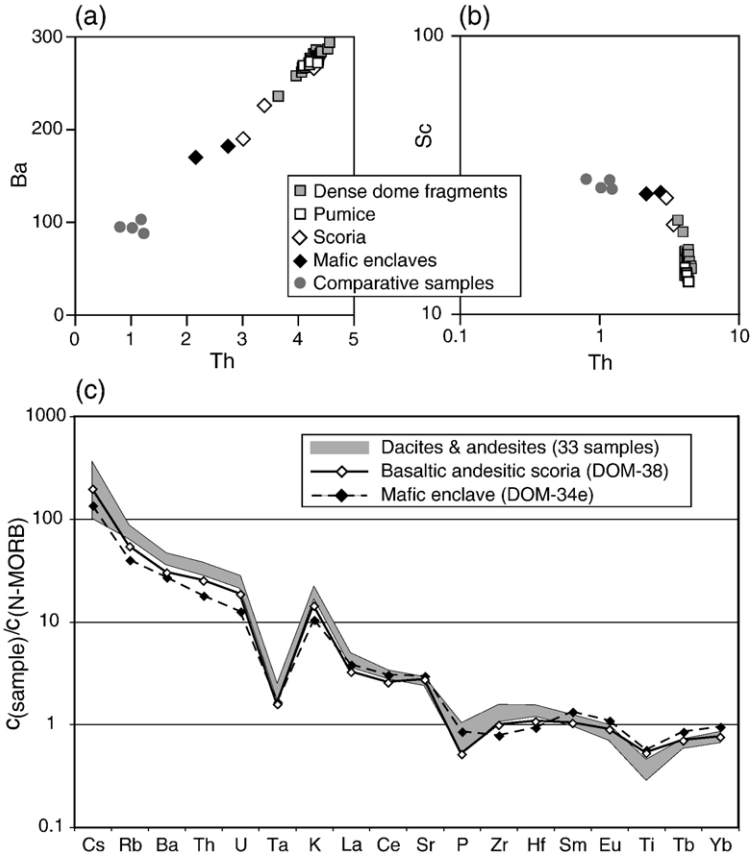

Fig. 6. (a), (b): Correlation diagrams of selected trace elements (in ppm) from whole-rock analyses of Plat Pays rocks. Comparative data are more primitive samples from Dominica (Joron, unpublished data) to illustrate the fractionation trends. Note that (b) has logarithmic scales and the steep decrease of Sc, indicative of clinopyroxene fractionation. (c) N-MORB normalized multi-element plot of Plat Pays rocks. N-MORB normalization data are from Sun and McDonough (1989).

will record the highest values of the closure pressure (P_c, i.e. the pressure at which the melt chemistry is quenched). The position of the two analyses displaced towards the Qz–Or join might be related to a non-equilibrium crystallization path (Cashman and Blundy, 2000).

6.5. Water contents

Melt water contents were estimated by comparing the compositions of natural glasses and phenocrysts with compositions produced experimentally under controlled conditions of T, P and f_{O2} . Experimental data on an andesite from Montagne Pelée (Martel et al., 1998), which is geochemically very similar to the Plat Pays rocks, have been used as a reference. Glass inclusion data were not used because of the unreliability of glass inclusions for the estimation of pre-eruptive melt water contents in eruption products from dome-forming eruptions (Martel et al., 2000) due to leakage and diffusion (e.g. Johnson et al., 1994), degassing of volatiles before entrapment (Macdonald et al., 2000), or secondary hydration. Unfortunately, the investigated pumices did not contain measurable glass inclusions.

Amphibole crystallization requires ~4% dissolved water in the melt (Merzbacher and Eggler, 1984). The enstatite content of orthopyroxene is also related to the melt water content at fixed P–f_{O2}. At 875 °C, P=2 kbar and ΔFMQ=+1.2 to +1.6, approximately the crystallization conditions of the Plat Pays silicic magmas (note that an independent pressure estimate for a dacite pumice from the Plat Pays complex of ~2 kbar is given in Gurenko et al. (2005)), a minimum melt water content of 5.5 wt.% is required in andesites and dacites (Fig. 9a). The average SiO_2 content of matrix glass from a Plat Pays andesite (DOM-14b$_1$) at 875 °C corresponds to a melt water content of ~5.5 wt.% as well (Fig. 9b). The range of glass compositions correspond to a range of melt water contents between 4.5 and 6 wt.%, but it has to be considered that melt water contents increase with

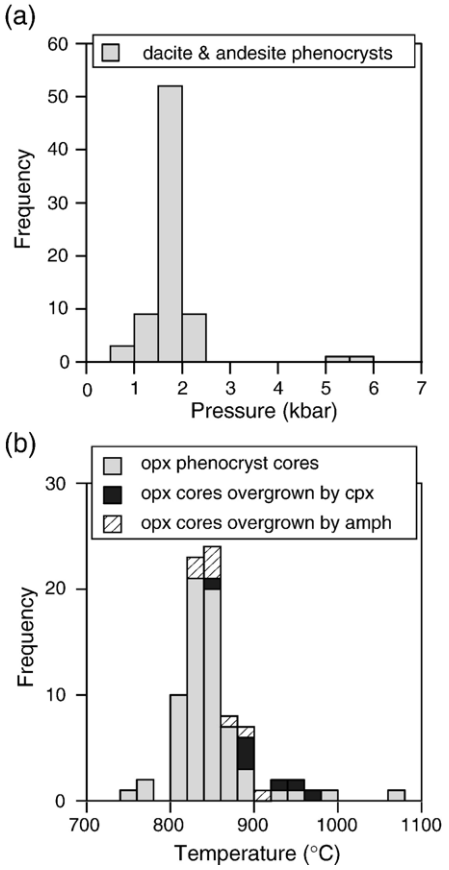

Fig. 7. (a) Histogram of pressures determined by Al-in-hornblende geobarometry (Johnson and Rutherford, 1989). Note that the two outliers were not considered in the average calculation. (b) Histogram of temperatures determined by QUILF orthopyroxene thermometry of phenocrysts in Plat Pays andesites and dacites (see text for details).

decreasing equilibration temperatures. At f_{O2} = ΔFMQ + 1.5, magnetite compositions indicate melt water contents >5.2 wt.% (Fig. 9c). In summary, the comparison with the experimental data on geochemically similar rocks reveal that pre-eruptive melt water contents are probably >5.2–5.5 wt.%, which is equivalent to a minimum P_{H2O} of 1.6 kbar, according to the solubility model of Newman and Lowenstern (2002). Although these estimates need experimental corroboration, in which phase stabilities, mineral and glass compositions of both dacitic and andesitic Plat Pays rocks in relation to changes in the intensive crystallization parameters would be more precisely determined (e.g. Rutherford et al., 1985; Martel et al., 1998), they suggest that the magmas were close to water-saturation at its storage pressures.

Maximum melt water contents can be derived from the maximum pressure estimate of 2.3 kbar. Assuming that the magmas are water-saturated and that other volatiles such as CO_2 are of minor importance, as suggested from near-infrared spectroscopy data in the case of Montagne Pelée (Martel et al., 2000) and FTIR data from Montserrat (Barclay et al., 1998), the melt water content would be ~ 6.5 wt.% H_2O at 2.3 kbar (calculated for rhyolite at 840 °C, using the VolatileCalc 1.1 software after Newman and Lowenstern (2002)). Thus, our best estimate of the pre-eruptive melt water content is between 5.2 and 6.5 wt.%.

7. Discussion

7.1. Crystallization environments of silicic magmas at the Plat Pays complex

The diversity in composition and textures of phenocryst phases in a same magma fragment or thin section underlines that the erupted silicic magmas represent a mixture of crystals that have experienced different thermal histories (Murphy et al., 1998). Therefore, dacites and andesites represent mixed hybrids. Evidences for mixing are numerous and include the presence of An-rich plagioclase cores that might derive from disaggregation of mafic enclaves at shallow levels and rare Al-rich amphiboles in some of the lava dome fragments that point to crystallization at elevated pressures. High-temperature (>900 °C) orthopyroxene cores can also be interpreted as remnants from incomplete mixtures of mafic and silicic magmas or as antecrysts (antecryst = crystal that is derived from an earlier evolutionary stage of the magmatic system but out of current equilibrium (Streck et al., 2005)). The rare low-temperature orthopyroxenes might be derived from cooler parts of the magma reservoir (Murphy et al., 2000). Abundant disequilibrium features observed at millimeter to micrometer scales are also consistent with mechanical mixing. For instance, resorption of orthopyroxene and crystallization of amphibole, consistent with an increase in the water content in the melt or in f_{O2} (Martel et al., 1999), only affected a few crystals in a given sample. Disequilibria are also indicated by the co-existence of amphibole with and without reaction rims, which are thought to result from decompression of the magma during ascent (Rutherford and Hill, 1993). Rounded amphiboles suggest episodes of resorption and dissolution that accompanied heating of magma. Similarly, the dusty sieve-textures in plagioclase can be explained by resorption and rapid re-growth (Murphy et al., 1998). Clinopyroxene rims on orthopyroxene can be explained by a local heating event, which raised the temperature of the pre-eruptive magma to the reaction boundary at which hornblende reacts to form clinopyroxene and melt (Rutherford and Devine, 1988; Devine et al.,

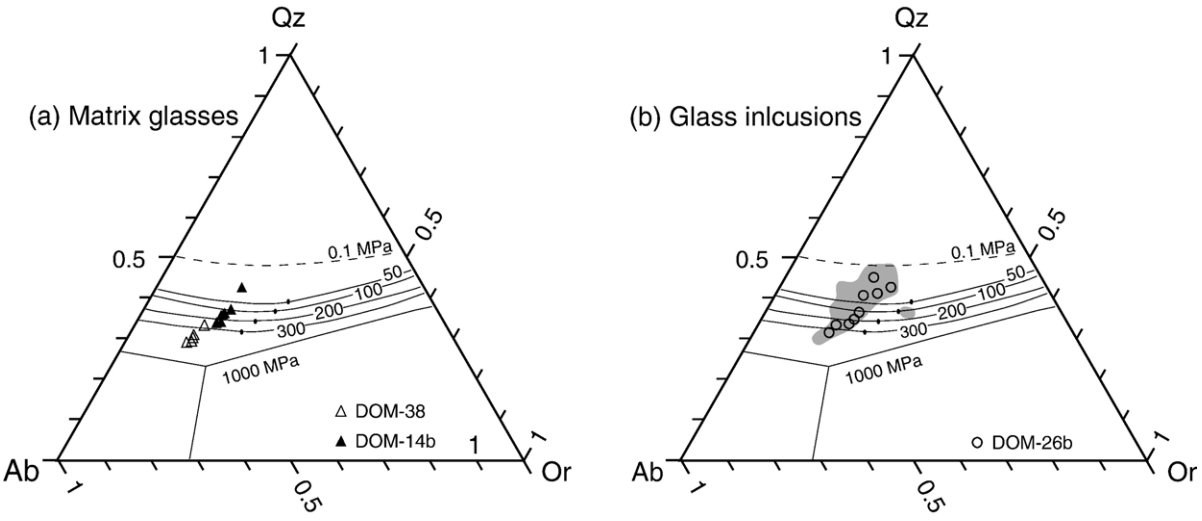

Fig. 8. Quartz–albite–orthoclase (Qz–Ab–Or) projection of glass analyses from Plat Pays rocks according to the projection scheme of Blundy and Cashman (2001). The plotting parameters Qz, Ab, Or are calculated from the CIPW norms of anhydrous glass analyses (for details of the projection scheme, see Blundy and Cashman (2001)). Cotectic lines and compositions of H_2O-saturated minima and eutectics in Qz–Ab–Or haplogranitic melts are after Blundy and Cashman (2001) and references therein. (a) Matrix glass from samples DOM-14b$_1$ (andesite) and DOM-38 (basaltic andesite). (b) Glass inclusions in sample DOM-26b (andesite). The grey area encompasses glass inclusion analyses from all investigated samples.

1998). The rare occurrence of quartz crystals is consistent with the calculated temperatures, as experimental data suggest that quartz appears first at 750 °C under H_2O-saturated conditions in dacite (Scaillet and Evans, 1999) and between 790 and 825 °C at pressures of 200–130 MPa in andesite (Rutherford and Devine, 2003).

Despite the mineralogical variability, there are no significant variations in bulk rock chemistry of the silicic samples with time. Minor compositional variations in the samples can be attributed to variable proportions of the constituent minerals. Therefore, the compositional monotony of the sample suite and the comparable mineralogical complexities in any given sample clearly suggest that long-term, time-dependent compositional variations in the magma system are of minor importance compared to the variability in the crystallization environments represented in the mineral assemblage of a particular sample. It is therefore useful to define a major crystallization environment of the silicic samples, which is defined by the presence of hornblende, temperatures in the range 800–880 °C, oxygen fugacities of +1.2 to +1.8 ΔFMQ and water contents between 5.2 and 6.5 wt.%. The water contents determined are in agreement with experimental data from Montagne Pelée andesite, where >6 wt.% H_2O is required to stabilize amphibole (Martel et al., 1999) and from Mt. Pinatubo dacite, where the absence of hornblende occurs below melt H_2O contents of 4–5 wt.% (Scaillet and Evans, 1999). The presence of clinopyroxene is also compatible with high water contents, as clinopyroxene was only present in H_2O-rich experimental charges <900 °C of andesite (Martel et al., 1999). The plagioclase zoning with elevated X_{An} is consistent with conditions close to or at H_2O saturation, since compositions of $X_{An}>60$ require relatively high temperatures and melt water content close to saturation (Scaillet and Evans, 1999).

Although significant crystallization is thought to have occurred within this dominant crystallization environment, there is also evidence of crystallization during final ascent of the silicic magmas. Decompression-driven crystallization is strongly indicated by the high Qz contents in the evolved silicic glasses, which can only be attained if the final crystallization pressure is low (Blundy and Cashman, 2001). Although Martel et al. (2000) suggested that highly differentiated glass inclusions (>77 wt.% SiO_2) result from devitrification and are therefore not representative of the pre-eruptive melt, the continuous trends on the Qz–Ab–Or diagram (Fig. 8) are consistent with continuously changing melt compositions recorded in response to slow magma ascent. The complex plagioclase zoning patterns combined with the absence of significant zoning in the mafic minerals are also in agreement with crystallization driven by decompression, since this crystallization environment is compatible with plagioclase growth largely in response to decompression inducing Ca/Na variation while Mg# stays relatively unchanged (Streck

et al., 2005). Following this argumentation, some of the plagioclase and orthopyroxene crystals must indeed have crystallized at a late stage during ascent, since the evolved melts were incorporated into them.

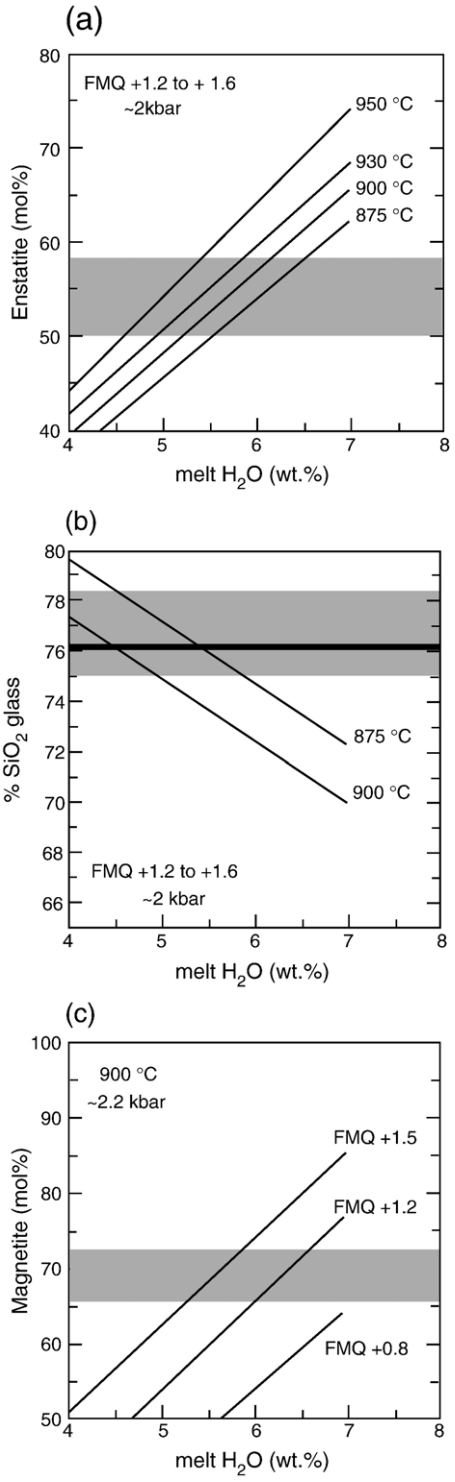

Fig. 9. Comparison of mineral chemical data from Plat Pays rocks with experimental data on Montagne Pelée andesites (after Martel et al., 1998). The shaded fields mark the predominant mineral and glass compositions of Plat Pays andesites/dacites. (a) Enstatite content in orthopyroxene vs. melt H_2O content; given the temperatures determined by QUILF (800–880 °C), a minimum water content of ~5.5 wt.% is indicated (b) weight percentage of SiO_2 in glass (only matrix glass) vs. melt H_2O content; thick black line marks the average of 5 matrix glass measurement in sample DOM-14b$_1$ (c) mole percentage of magnetite (in titanomagnetite) vs. melt H_2O content.

7.2. Parental magmatic liquids of basaltic andesitic to basaltic composition

Evidence for more mafic precursor magmas to the andesites and dacites includes the presence of xenocrysts and disequilibrium features in the latter (see above), and is manifested in the mafic enclaves and an occurrence of scoria of basaltic andesitic composition (sample DOM-38). The crenulate contacts and the presence of host-derived xenocrysts, such as the brown magnesio-hornblendes with Al_2O_3 ~7 wt.%, in the mafic enclaves are characteristic of magmatic mafic inclusions which have been quenched in a cooler silicic liquid (Bacon, 1986). Comparable whole-rock chemistries and normalized trace element patterns of the mafic enclaves and the scoria DOM-38 point to a common mafic magma composition. However, some distinct mineralogical and petrological differences might be present, as exemplified for the enclave DOM-8d. There, the growth of amphibole at the expense of pyroxenes is evidence for an increase of water-pressure during crystallization. T–f_{O2} re-equilibration of xenoliths with enclosing rocks after mixing is indicated by correspondence in physical conditions between xenolith and host rock data. It seems unlikely that this xenolith represents a hydrous magma that never reached the surface because of the chemical similarities with the scoria and because amphibole is probably not a liquidus phase but rather a reaction product between a liquid and early formed crystals during a cooling stage (Coulon et al., 1984). Although it cannot be excluded that this enclave represents a cumulate crystallizing in a marginal solidification zone (Langmuir, 1989), the continuously changing amphibole compositions (Fig. 4) are more compatible with crystallization at variable depths during ascent (Arculus and Wills, 1980). Growth of amphibole during magma ascent is only possible at pressures above ~ 1 kbar, suggesting that amphibole phenocrysts started to crystallize at elevated pressures. The acicular morphology of the amphiboles suggests rapid crystallization of a quenched liquid

(Coulon et al., 1984) and implies that the intruding mafic magmas were dominantly in a liquid state.

Similar trace element patterns and characteristic trends on two-element plots (Fig. 6) are consistent with a fractional crystallization relationship and suggest a genetic link between the mafic enclaves and the basaltic andesite scoria on the one hand and the andesites/dacites on the other hand. In addition to the variable proportions of constituent minerals, variable amounts of mafic magma hybridization of andesitic magma can also explain the minor compositional variations in the dacite/andesite samples. Since it appears that the enclaves were hydrated and partly re-equilibrated in contact with the silicic resident magma, the scoria (DOM-38) is a more reliable indicator of the predominant T–f_{O2} relationships (~1060 °C, f_{O2}=+1.6 to +2.0 ΔFMQ) in the more mafic magmas of Plat Pays. Additional qualitative information can be gained from the highly calcic plagioclase cores in the silicic rocks that are thought to reflect high water contents in the mafic magma they crystallized from (Sisson and Grove, 1993).

Chemical differences between amphibole populations in the dacites and the mafic enclaves can be related to higher temperature, higher crystallization pressure or the SiO_2-saturation of the melt (Johnson and Rutherford, 1989; Scaillet and Evans, 1999; Rutherford and Devine, 2003). A comparison of the Al^{VI} contents of the amphiboles with experimental compositions produced at 200 and 250 MPa (Rutherford and Devine, 2003) reveals that Al^{VI} in the amphiboles of the mafic enclaves is significantly higher than in the bulk of magnesio-hornblendes from the dacites and consistent with crystallization at P>250 MPa (Fig. 4). Therefore, we conclude that the amphiboles of the mafic enclaves represent crystallization at elevated pressures compared to the bulk andesites. This interpretation agrees well with the presence of high-Al clinopyroxene cores in some of them.

Further constraints on the crystallization of ferromagnesian minerals can be derived from equilibrium relationships of the ratio Fe/Mg between melt and silicate minerals (Streck et al., 2005). Fig. 10 shows the Mg# clinopyroxenes plotted versus the Mg# of whole-rock or glass together with two curves for pyroxene-melt distribution coefficients K_d^{Fe-Mg} using values of 0.26 and 0.3 (Sisson and Grove, 1993; Streck et al., 2005). The K_d values allow calculating Fe/Mg and Mg# of a melt coexisting with a chosen clinopyroxene composition. For clinopyroxenes from the mafic enclaves, calculated Fe/Mg reaches values down to 0.5, which translates into a maximum Mg# of

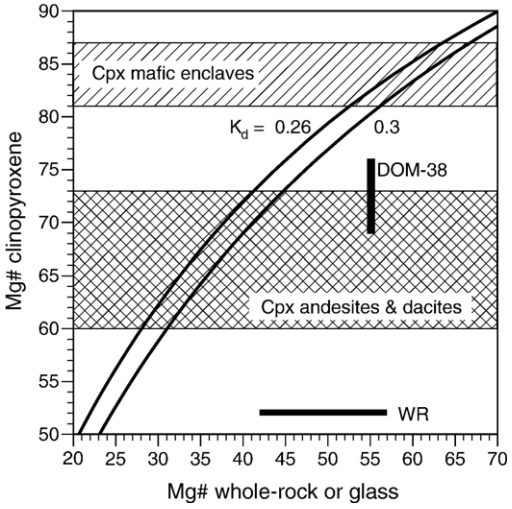

Fig. 10. Clinopyroxene Mg# vs. Mg# of whole rock or glass. Values for the Fe–Mg equilibrium distribution coefficient are from Sisson and Grove (1993).

67 (Fig. 10). This is significantly more magnesian than the most Mg-rich erupted rock present, including the basaltic andesite scoria with Mg#=56. Therefore, we conclude that, at depth, magmas were more mafic (i.e. basaltic) than magmas erupted as scoria or incorporated as enclaves. It is also noteworthy that the calculated Mg# of the melts in equilibrium with the clinopyroxene crystals in the silicic rocks yields values of 28–41, which tends to be lower than the Mg# of the whole-rocks. This strengthens the point that the silicic rocks are hybrids between intruding mafic and resident silicic magmas.

In a recent geochemical study, Lindsay et al. (2005) argue that the scoriaceous deposits from which sample DOM-38 was collected can be correlated to scoria deposits from the Morne Anglais complex in the north of the Plat Pays complex. As outlined above, the sample is compositionally very similar to the Plat Pays mafic enclaves, both in terms of major and trace elements. It also plots on the compositional trends established for the Plat Pays rocks (Figs. 5 and 6), consistent with a co-genetic origin. Even if the origin of this sample is considered as doubtful, the presence of mafic enclaves, the petrographic disequilibrium features (Fig. 2) and the calculation of the Mg# of melts coexisting with clinopyroxene from the enclaves provide clear evidence for the presence of more mafic magmas at some point in the evolution of the Plat Pays complex. T–f_{O2} conditions determined for the mafic enclaves and DOM-38 overlap, so that the values determined for DOM-38 can still be considered as representative for

those mafic magmas. Therefore, the main conclusions of this study remain valid.

7.3. Magma dynamics and magma storage

An important question regarding the magma reservoir at the Plat Pays complex is whether there is long-lived reservoir present or whether there are only small reservoirs established at each eruptive cycle. This has important implications for possible eruptions, since in the former case a relatively large magma volume might be activated in an eruption. As demonstrated above, mafic and silicic magmas that partly mixed were involved in the magma generation. A coupling of the mafic and silicic parts at Plat Pays, rather similar to a model proposed by Pichavant et al. (2002) for Montagne Pelée, is supported by the fractional crystallization relationship deduced from trace element data. Magmas appear to have crystallized over a large pressure range, starting perhaps at lower crustal depth as indicated by the Al-in-hornblende geobarometry. Since amphibole cannot survive for more than a few days outside its stability field (Rutherford and Hill, 1993), magma must have been stored at various levels within the sub-volcanic system, partly within the amphibole stability field (no reaction rims), some outside at shallower levels (with reactions rims). This is consistent with mixing textures and variable grain size observed. In fact, mixing of magmas from different storage levels is inevitable if the magma conduit remains at least partially full between eruptions (Blundy and Cashman, 2001). A fairly shallow major magma storage region at depths of 4–9 km from which magma degassing could have occurred is supported with the very low total volatile contents in most of the melt inclusions. It is also in agreement with the dominant dome-forming eruption style of Plat Pays, which requires open-system gas loss (Villemant et al., 1996; Villemant and Boudon, 1998). All dome fragments investigated are dense and crystal-rich, and the calculated temperatures and oxygen fugacities are identical within error for the different samples, apparently independent of the relative ages. Although crystallization by decompression is a viable mechanism to generate crystal-rich magmas (Métrich et al., 2001) and the highly evolved glass compositions of the Plat Pays rocks are clearly indicative of crystallization at very shallow depths, the high total phenocrysts abundance (>45%) suggests a high crystal content of the pre-eruptive magma (Rutherford and Devine, 2003). Additionally, the limited range in bulk-rock chemistry points towards similar magma chemistries, modified only by variations in the influx of more mafic melts. The relatively low temperatures of ~840 °C compared to the experimentally determined water-saturated liquidus of andesite (1050 °C at 1.5 kbar; Barclay et al., 1998) and the high crystallinities characterized by a high proportion of large crystals, reflecting extensive crystallization, are indicative of a long cooling history. These features are consistent with a long-lived magma reservoir that might have existed in the crust from >100 ka to the most recent eruptions. Magma residence times within arc crust in a similar order of magnitude (~ 60 ka) were demonstrated by U–Th isochron dating for instance at Soufrière, St. Vincent (Heath et al., 1998b). In summary, the mineralogy and the textures suggest a mixing together of phenocrysts and non-uniform re-heating and remobilization of resident magma with near-identical pre-eruptive conditions by intrusion of hotter, mafic melts. However, the main impact of the mafic melts is the supply of heat, since the small changes in overall magma chemistry and the small percentage of relatively intact enclaves do not support extensive mingling. As postulated for Montserrat (Murphy et al., 2000), the influx of mafic magma might also trigger eruptions at Plat Pays, so that the ascent of mafic magma could be a useful warning, if detected.

7.4. Comparison of crystallization conditions with other volcanoes from the Lesser Antilles arc

A comparison of petrological data from Plat Pays with other volcanoes of the Lesser Antilles arc (Fig. 11) shows that temperatures and oxygen fugacities of the Plat Pays resident silicic magma are comparable to those from Montagne Pelée (875–900 °C, f_{O2} ~ΔFMQ +1.2 to +1.6; Martel et al., 1998, Pichavant et al., 2002) and Soufrière Hills, Montserrat (810–880 °C, f_{O2} ~ΔFMQ +1.5 to +2.1; Murphy et al., 1998, 2000). Higher temperatures of the andesitic resident magma were determined for the Soufrière volcano on St. Vincent (T=1000 °C; Heath et al., 1998a) and La Soufrière on Guadeloupe (T=950 °C, Semet et al., unpublished data) where, in contrast to Plat Pays, amphibole is lacking, in accordance with the stability limit of amphibole. Dacites from Pitons du Carbet, Martinique, gave lower temperatures at comparable oxygen fugacities (T=750 °C, f_{O2}>ΔFMQ+0.8; D'Arco et al., 1981). Crystallization pressure of the Plat Pays magmas is lower than at Soufrière St. Vincent (~3 kbar; Heath et al., 1998a) and Pitons du Carbet (2.3–4.5 kbar, D'Arco et al., 1981), but similar to Montagne Pelée (2 ± 0.5 kbar, Martel et al., 1998) and La Soufrière, Guadeloupe (1.8 kbar, Semet et al., unpublished

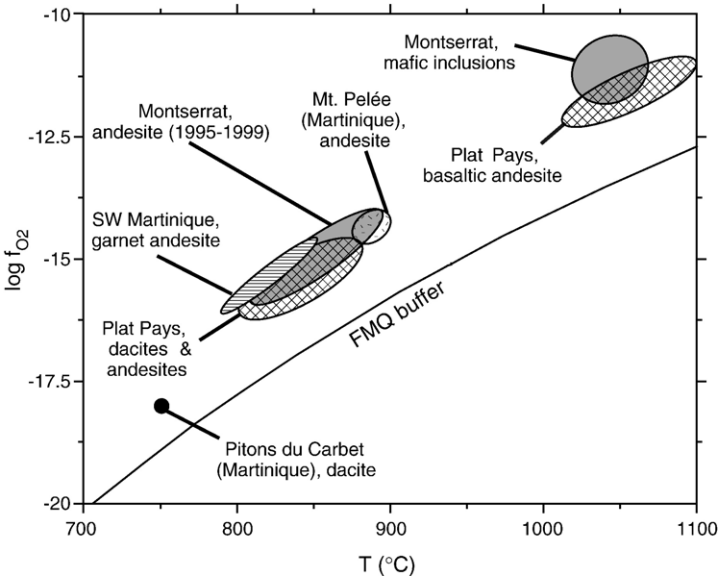

Fig. 11. T–f_{O2} diagram of Plat Pays rocks in comparison with published data from andesitic and dacitic rocks of the Lesser Antilles arc. FMQ is the buffer reaction fayalite+O_2=magnetite+SiO_2. Comparative data sources: Soufrière Hills, Montserrat: Murphy et al. (2000); Montagne Pelée: Martel et al. (1998), Pichavant et al. (2002); Pitons du Carbet: D'Arco et al. (1981); SW Martinique: Maury et al. (1985).

data). Significantly higher total pressures of 6–11 kbar, however, were estimated for andesites and dacites on Martinique (Coulon et al., 1984). Estimated melt water contents of the Plat Pays magmas are slightly elevated compared to Soufriere Hills magmas (4.7 wt.%, Devine et al., 1998), but compare well with andesitic magmas from Montagne Pelée (5.3–6.3 wt.%, Martel et al., 2000). It is likely that the upper parts of the Plat Pays magma reservoir were saturated with a H_2O-rich vapor phase. In summary, temperatures and oxygen fugacities of Plat Pays silicic magmas are in the middle range for the Lesser Antilles arc, whereas water contents are at the upper end and total pressures at the lower end of the within arc variability.

The mafic magmas from Plat Pays show some similarity to Soufrière, St. Vincent, where basaltic andesites equilibrated at 1050 °C (Heath et al., 1998a), and to the South Soufriere Hills basalt from Montserrat with temperatures of 1050–1080 °C (Murphy et al., 2000). Calculations of intensive parameters from mafic enclaves yielded $T \geq 1050$ °C and f_{O2}=ΔFMQ +2.0 to +2.8 in the current Montserrat andesite (Murphy et al., 2000) and 1090 °C in xenoliths from Montagne Pelée (Fichaut et al., 1989), also roughly equivalent to the conditions estimated for the mafic Plat Pays magmas. The postulated presence of basaltic magmas at Plat Pays with high water contents could be comparable to the situation at Montagne Pelée, where a magma chamber fed by an evolved basaltic liquid (Mg#=55–60) with high melt H_2O (5–6 wt.%) was recognized (Pichavant et al., 2002). Thus, the mafic magmas of Plat Pays, albeit volumetrically of minor importance, resemble very much, both in geochemistry and crystallization parameters, their counterparts from other islands of the arc.

8. Conclusions

During the last ~100 ka, the Plat Pays volcanic complex in southern Dominica was fed by mafic magmas of basaltic andesitic to basaltic composition that intruded a long-lived, highly crystallized silicic magma reservoir. The mafic magmas started crystallization at elevated depth >10 km at temperatures around 1060 °C. They partially mixed with andesitic to dacitic magmas in a relatively shallow magma reservoir at 1.1 to 2.3 kbar total pressure. In the silicic magma reservoir, a dominant crystallization environment can be defined, which is characterized by moderately oxidizing conditions at ΔFMQ +1.5 ± 0.3 and temperatures of 800–880 °C. Estimated melt water contents of 5.2 to 6.5 wt.% suggest conditions at or close to H_2O-saturation in the reservoir. Decompression-driven crystallization and degassing during final ascent lead to the formation of SiO_2-rich, volatile-poor residual liquids. The inferred magma storage conditions of the Plat Pays volcano are very similar to those at the Soufriere Hills volcano, Montserrat, and Montagne Pelée, Martinique, and may be useful in evaluating the evolution of possible future eruptions.

Acknowledgements

Frédéric Couffignal and Michel Fialin are thanked for help with microprobe work. Critical comments by Andrea Di Muro greatly improved an earlier version of the manuscript. We thank M. Rutherford and an anonymous referee for their constructive reviews and B. Marsh for editorial handling. Funding for this work from the EU Volcano Dynamics Research Training Network and the French PNRN (INSU-CNRS) Research Program is gratefully acknowledged.

References

Andersen, D.J., Lindsley, D.H., Davidson, P.M., 1993. QUILF: a PASCAL program to assess equilibria among Fe–Mg–Ti oxides, pyroxenes, olivine and quartz. Comput. Geosci. 19, 1333–1350.

Anderson, J.L., Smith, D.R., 1995. The effects of temperature and f_{O2} on the Al-in-hornblende barometer. Am. Mineral. 80, 549–559.

Arculus, R.J., Wills, K.J.A., 1980. The Petrology of plutonic blocks and inclusions from the Lesser Antilles Arc. J. Petrol. 21, 743–799.

Bacon, C., 1986. Magmatic inclusions in silicic and intermediate volcanic rocks. J. Geophys. Res. 91, 6091–6112.

Barclay, J., Rutherford, M.J., Carroll, M.R., Murphy, M.D., Devine, J.D., Gardner, J., Sparks, R.S.J., 1998. Experimental phase equilibria constraints on pre-eruptive storage conditions of the Soufriere Hills magma. Geophys. Res. Lett. 25, 3437–3440.

Blundy, J., Cashman, K., 2001. Ascent-driven crystallisation of dacite magmas at Mount St. Helens, 1980–1986. Contrib. Mineral. Petrol. 140, 631–650.

Brown, G.M., Holland, J.G., Sigurdsson, H., Tomblin, J.F., Arculus, R.J., 1977. Geochemistry of the Lesser Antilles volcanic island arc. Geochim. Cosmochim. Acta 41, 785–801.

Cashman, K., Blundy, J., 2000. Degassing and crystallization of ascending andesite and dacite. Philos. Trans. R. Soc. Lond., A 358, 1487–1513.

Coulon, C., Clocchiatti, R., Maury, R.C., Westercamp, D., 1984. Petrology of basaltic xenoliths in andesitic to dacitic host lavas from Martinique (Lesser Antilles): evidence for magma mixing. Bull. Volcanol. 47, 705–734.

D'Arco, P., Maury, R.C., Westercamp, D., 1981. Geothermometry and geobarometry of a cummingtonite-bearing dacite from Martinique, Lesser Antilles. Contrib. Mineral. Petrol. 77, 177–184.

Deplus, C., Le Friant, A., Boudon, G., Komorowski, J.-C., Villemant, B., Harford, C., Ségoufin, J., Cheminée, J.-L., 2001. Submarine evidence for large-scale debris avalanches in the Lesser Antilles Arc. Earth Planet. Sci. Lett. 192, 145–157.

Devine, J.D., Gardner, J.E., Brack, H.P., Layne, G.D., Rutherford, M.J., 1995. Comparison of microanalytical methods for estimating H_2O contents of silicic volcanic glasses. Am. Mineral. 80, 319–328.

Devine, J.D., Murphy, M.D., Rutherford, M.J., Barclay, J., Sparks, R.S.J., Carroll, M.R., Young, S.R., Gardner, J.E., 1998. Petrologic evidence for pre-eruptive pressure-temperature conditions, and recent reheating, of andesitic magma erupting at the Soufriere Hills Volcano, Montserrat, W.I. Geophys. Res. Lett. 25, 3669–3672.

Druitt, T.H., Kokelaar, B.P., 2002. The eruption of Soufriere Hills volcano, Montserrat, from 1995–1999. Geol. Soc. Lond. Mem. 21 (645 pp.)

Fichaut, M., Marcelot, G., Clocchiatti, R., 1989. Magmatology of Mt. Pelée (Martinique, F.W.I.): II. Petrology of gabbroic and dioritic cumulates. J. Volcanol. Geotherm. Res. 38, 171–187.

Gurenko, A.A., Trumbull, R.B., Thomas, R., Lindsay, J.M., 2004. Tracing source components in dacitic magmas (Dominica, Lesser Antilles): data from melt inclusions. Beih. Z. Eur. J. Mineral. 16 (1), 51.

Gurenko, A.A., Trumbull, R.B., Thomas, R., Lindsay, J.M., 2005. A melt inclusion record of volatiles, trace elements and Li-B isotope variations in a single magma system from the Plat Pays Volcanic Complex, Dominica, Lesser Antilles. J. Petrol. 46, 2495–2526.

Hammer, J.E., Cashman, K.V., Voight, B., 2000. Magmatic processes revealed by textural and compositional trends in Merapi dome lavas. J. Volcanol. Geotherm. Res. 100, 165–192.

Heath, E., Macdonald, R., Belkin, H., Hawkesworth, C., Sigurdsson, H., 1998a. Magmagenesis at Soufriere Volcano, St Vincent, Lesser Antilles Arc. J. Petrol. 39, 1721–1764.

Heath, E., Turner, S.P., Macdonald, R., Hawkesworth, C.J., van Calsteren, P., 1998b. Long magma residence times at an island arc volcano (Soufriere, St. Vincent) in the Lesser Antilles: evidence from ^{238}U–^{230}Th isochron dating. Earth Planet. Sci. Lett. 160, 49–63.

Holland, T.J., Blundy, J.D., 1994. Non-ideal interactions in calcic amphiboles and their bearing on amphibole-plagioclase thermometry. Contrib. Mineral. Petrol. 116, 431–447.

Irvine, T.N., Baragar, W.R.A., 1971. A guide to the chemical classification of the common volcanic rocks. Can. J. Earth Sci. 8, 523–548.

Johnson, M.C., Rutherford, M.J., 1989. Experimental calibration of the aluminum-in-hornblende geobarometer with application to Long Valley caldera (California) volcanic rocks. Geology 17, 837–841.

Johnson, M.C., Anderson, A.T., Rutherford, M.J., 1994. Pre-eruptive volatile contents of magmas. In: Carroll, M.R., Holloway, J.R. (Eds.), Volatiles in Magmas. Reviews in Mineralogy. Mineralogical Society of America, pp. 281–330.

Joron, J.-L., Treuil, M., Raimbault, L., 1997. Activation analysis as a geochemical tool: statement of capabilities for geochemical trace element studies. J. Radioanal. Nucl. Chem. 216, 229–235.

Langmuir, C.H., 1989. Geochemical consequences of in situ crystallization. Nature 340, 199–205.

Lacroix, A., 1904. La Montagne Pelée et ses Eruptions. Masson et Cie, Paris. 662 pp.

Le Friant, A., Boudon, G., Komorowski, J.-C., Deplus, C., 2002. L'île de la Dominique, à l'origine des avalanches de débris les plus volumineuses de l'arc des Petites Antilles. C. R. Geosci. 334, 235–243.

Leake, B.E., et al., 1997. Nomenclature of amphiboles: report of the subcommittee on amphiboles of the International Mineralogical Association, Commission on new minerals and mineral names. Can. Mineral. 35, 219–246.

Lindsay, J.M., Stasiuk, M.V., Shepherd, J.B., 2003. Geological history and potential hazards of the Late-Pleistocene to Recent Plat Pays volcanic complex, Dominica, Lesser Antilles. Bull. Volcanol. 65, 201–220.

Lindsay, J.M., Trumbull, R.B., Siebel, W., 2003. Geochemistry and petrogenesis of late Pleistocene to recent volcanism in Southern Dominica, Lesser Antilles. J. Volcanol. Geotherm. Res. 148, 254–294.

Macdonald, R., Hawkesworth, C., Heath, E., 2000. The Lesser Antilles volcanic chain: a study in arc magmatism. Earth Sci. Rev. 49, 1–76.

Martel, C., Pichavant, M., Bourdier, J.-L., Traineau, H., Holtz, F., Scaillet, B., 1998. Magma storage conditions and control of eruption regime in silicic volcanoes: experimental evidence from Mt. Pelée. Earth Planet. Sci. Lett. 156, 89–99.

Martel, C., Pichavant, M., Holtz, F., Scaillet, B., Bourdier, J.-L., Traineau, H., 1999. Effects of f_{O2} and H_2O on andesite phase relations between 2 and 4 kbar. J. Geophys. Res. 104 (B12), 29453–29470.

Martel, C., Bourdier, J.-L., Pichavant, M., Traineau, H., 2000. Textures, water content and degassing of silicic andesites from recent plinian and dome-forming eruptions at Mount Pelée volcano (Martinique, Lesser Antilles arc). J. Volcanol. Geotherm. Res. 96, 191–206.

Maury, R.C., Clocchiatti, R., Coulon, C., D'Arco, P., Westercamp, D., 1985. Signification du Grenat et de la Cordiérite dans les laves du Sud-Ouest Martiniquais. Bull. Mineral. 108, 63–79.

Merzbacher, C., Eggler, D.H., 1984. A magmatic geohygrometer: application to Mount St. Helens and other dacitic magmas. Geology 12, 587–590.

Métrich, N., Bertagnini, A., Landi, P., Rosi, M., 2001. Crystallization driven by decompression and water loss at Stromboli volcano (Aeolian island). Italy. J. Petrol. 42, 1471–1490.

Middlemost, E.A.K., 1989. Iron oxidation ratios, norms and the classification of volcanic rocks. Chem. Geol. 77, 19–26.

Morimoto, N., Fabrie, J., Ferguson, A.K., Ginzburg, I.V., Ross, M., Seifert, F.A., Zussman, J., Aoki, K., Gottardi, G., 1988. Nomenclature of pyroxenes. Mineral. Mag. 52, 535–550.

Murphy, M.D., Sparks, R.S.J., Barclay, J., Carroll, M.R., Lejeune, A.-M., Brewer, T.S., Macdonald, R., Black, S., Young, S., 1998. The role of magma mixing in triggering the current eruption at the Soufrière Hills volcano, Montserrat, West Indies. Geophys. Res. Lett. 25, 3433–3436.

Murphy, M.D., Sparks, R.S.J., Barclay, J., Carroll, M.R., Brewer, T.S., 2000. Remobilization of andesite magma by intrusion of mafic magma at the Soufrière Hills Volcano, Montserrat, West Indies. J. Petrol. 41, 21–42.

Newman, S., Lowenstern, J.B., 2002. VolatileCalc: a silicate melt–H2O–CO2 solution model written in visual basic for excel. Comput. Geosci. 28, 597–604.

Perret, F.A., 1937. The Eruptions of Mt. Pelée 1929–1932. Carnegie Inst. Washington Publ., vol. 458. 126 pp.

Pichavant, M., Martel, C., Bourdier, J.-L., Scaillet, B., 2002. Physical conditions, structure, and dynamics of a zoned magma chamber: Mount Pelée (Martinique, Lesser Antilles Arc). J. Geophys. Res. 107 (B5), 2093.

Pouchou, J.-L., Pichoir, F., 1985. "PAP" (phi–rho–*Z*) procedure for improved quantitative microanalysis. In: Armstrong, J.T. (Ed.), Microbeam Analysis. San Francisco Press, San Francisco, California, pp. 104–106.

Rutherford, M.J., Devine, J.D., 1988. The May 18, 1980, eruption of Mount St. Helens: 3. Stability and chemistry of amphibole in the magma chamber. J. Geophys. Res. 93 (B10), 11949–11959.

Rutherford, M.J., Devine, J.D., 2003. Magmatic conditions and magma ascent as indicated by hornblende phase equilibria and reactions in the 1995–2002 Soufrière Hills magma. J. Petrol. 44, 1433–1454.

Rutherford, M.J., Hill, P.M., 1993. Magma ascent rates from amphibole breakdown: an experimental study applied to the 1980–1986 Mount St. Helens eruptions. J. Geophys. Res. 98 (B11), 19667–19685.

Rutherford, M.J., Sigurdsson, H., Carey, S., 1985. The May 18, 1980 eruption of Mount St. Helens, 1. Melt composition and experimental phase equilibria. J. Geophys. Res. 90, 2929–2947.

Scaillet, B., Evans, B.W., 1999. The 15 June 1991 eruption of Mount Pinatubo, I, Phase equilibria and pre-eruption P–T–f_{O2}–H_2O conditions of the dacite magma. J. Petrol. 40, 381–411.

Sisson, T.W., Grove, T.L., 1993. Experimental investigations of the role of H_2O in calc-alkaline differentiation and subduction zone magmatism. Contrib. Mineral. Petrol. 113, 143–166.

Sun, S.-S., McDonough, W.F., 1989. Chemical and isotopic systematics of oceanic basalts: implications for mantle composition and processes. In: Saunders, A.D., Norry, M.J. (Eds.), Magmatism in Ocean Basins, Geological Society, London, Special Publication, vol. 42, pp. 313–345.

Stasiuk, M.V., Shepherd, J.B., Latchman, J., Lindsay, J.M., 2002. Intrusion-induced caldera fault slip imaged by shallow seismicity on Dominica, West Indies, 1998–2000. Seismol. Res. Lett. 73, 242.

Streck, M.J., Dungan, M.A., Bussy, F., Malavassi, E., 2005. Mineral inventory of continuously erupting basaltic andesites at Arenal volcano, Costa Rica: implications for interpreting monotonous, crystal-rich, mafic arc stratigraphies. J. Volcanol. Geotherm. Res. 140, 133–155.

Villemant, B., Boudon, G., 1998. Transition from dome-forming to plinian eruptive styles controlled by H_2O and Cl degassing. Nature 392, 65–69.

Villemant, B., Boudon, G., Komorowski, J.-C., 1996. U-series disequilibrium in arc magmas induced by water–magma interaction. Earth Planet. Sci. Lett. 140, 259–267.

Wadge, G., 1985. Morne Patates volcano, southern Dominica, Lesser Antilles. Geol. Mag. 122, 253–260.

White, W.M., Dupré, B., 1986. Sediment subduction and magma genesis in the Lesser Antilles: isotopic and trace element constraints. J. Geophys. Res. 91 (B6), 5927–5941.

Young, S.R., Sparks, R.S.J., Aspinall, W.P., Lynch, L.L., Miller, A.D., Robertson, R.E.A., Shepherd, J., 1998. Overview of the eruption of the Soufrière Hills volcano, Montserrat, July 18, 1995 to December 1997. Geophys. Res. Lett. 25, 3389–3392.